APPLIED ORGANOMETALLIC CHEMISTRY
Appl. Organometal. Chem. 2006; **20**: 51–69
Materials, Nanoscience and Catalysis AOC
Published online 21 November 2005 in Wiley InterScience (www.interscience.wiley.com). DOI:10.1002/aoc.1010

Reactions of $[Ru(CO)_3Cl_2]_2$ with aromatic nitrogen donor ligands in alcoholic media

M. Andreina Moreno, Matti Haukka*, Mirja Kallinen and Tapani A. Pakkanen

Department of Chemistry, University of Joensuu, PO Box 111, FIN-80101 Joensuu, Finland

Received 20 July 2005; Accepted 29 September 2005

The reactions of mono- and bidentate aromatic nitrogen-containing ligands with $[Ru(CO)_3Cl_2]_2$ in alcohols have been studied. In alcoholic media the nitrogen ligands act as bases promoting acidic behaviour of alcohols and the formation of alkoxy carbonyls $[Ru(N–N)(CO)_2Cl(COOR)]$ and $[Ru(N)_2(CO)_2Cl(COOR)]$. Other products are monomers of type $[Ru(N)(CO)_3Cl_2]$, bridged complexes such as $[Ru(CO)_3Cl_2]_2(N)$, and ion pairs of the type $[Ru(CO)_3Cl_3]^-$ $[Ru(N–N)(CO)_3Cl]^+$ (N–N = chelating aromatic nitrogen ligand, N = non-chelating or bridging ligand). The reaction and the product distribution can be controlled by adjusting the reaction stoichiometry. The reactivity of the new ruthenium complexes was tested in 1-hexene hydroformylation. The activity can be associated with the degree of stability of the complexes and the ruthenium–ligand interaction. Chelating or bridging nitrogen ligands suppresses the activity strongly compared with the bare ruthenium carbonyl chloride, while the decrease in activity is less pronounced with monodentate ligands. A plausible catalytic cycle is proposed and discussed in terms of ligand–ruthenium interactions. The reactivity of the ligands as well as the catalytic cycle was studied in detail using the computational DFT methods.

KEYWORDS: ruthenium complexes; pyridine; pyrazine; bipyridine; phenanthroline

INTRODUCTION

Ruthenium polypyridines display excellent electrochemical and photochemical properties[1,2] with applications in optics and solar cells.[3–5] Other ruthenium nitrogen-containing complexes, particularly those with nitrogen-based ligand bridges between divalent ruthenium centers,[6,7] have been studied for the purpose of establishing the nature of electronic phenomena such as π-back-bonding and electron transfer.[8–10] Such properties make them potential components in the field of nanoelectronic devices and molecular wires.[11,12]

Catalytic applications of these complexes include, for example, epoxidation of cyclohexene,[13] cyclopropanation of styrene,[14] water gas shift reaction[15] and carbon dioxide reduction.[16,17] A more recent application of these compounds is as nitric oxide (NO^-) radical releasers that could participate in biological processes like modulation of immune and endocrine response.[18,19]

*Correspondence to: Matti Haukka, Department of Chemistry, University of Joensuu, PO Box 111, FIN-80101 Joensuu, Finland.
E-mail: matti.haukka@joensuu.fi
Contract/grant sponsor: Academy of Finland.

Although the chemistry related to ruthenium polypyridine complexes has been widely studied, the behavior of these particular ligands in alcoholic media is less well known. We have previously shown that, in the presence of aromatic nitrogen ligands, alcohols can participate actively in complex formation.[20–22] In this work we investigated a series of reactions of several monodentate and bidentate nitrogen donor ligands with $[Ru(CO)_3Cl_2]_2$ in alcoholic media, focusing on the reaction mechanisms, the acid character of the solvents and the basic character of the selected ligands. We also studied the influence of the stoichiometry on the control of the products. The reactivity and stability of the ligands and their corresponding metal complexes is also investigated. According to these results we propose a catalytic cycle supported by computational methods. The studied aromatic nitrogen ligands are summarized in Scheme 1.

RESULTS AND DISCUSSION

Reaction route studies

We studied the reactions of $[Ru(CO)_3Cl_2]_2$ with various aromatic nitrogen ligands, including pyrazine, pyridine and

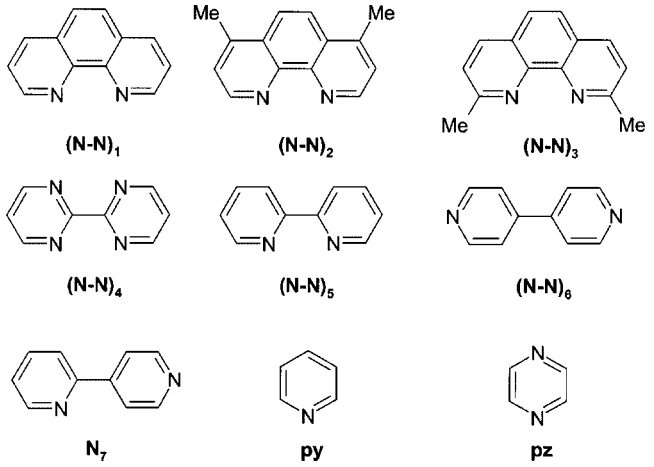

Scheme 1. Selected aromatic nitrogen donor ligands.

several polypyridines. When $[Ru(CO)_3Cl_2]_2$ reacts it typically breaks down into monomeric products. This reaction can be either symmetrical or asymmetrical depending on the solvents and other reagents available.

Formation of solvent intermediates

In the case of symmetrical cleavage, $[Ru(CO)_3Cl_2]_2$ produces in principle two equal units of $[Ru(CO)_3Cl_2]$. If the system includes coordinating solvents, such as acetonitrile, alcohols or THF, the vacancy in the ruthenium's coordination sphere will be filled with solvent, leading to $[Ru(CO)_3Cl_2(solv)]$. The symmetric cleavage of this dimer has previously been suggested in the literature by several authors. For example, formation of $[Ru(CO)_3Cl_2(EtOH)]$ has been verified by osmometric methods.[23] Similarly, the THF derivative $[Ru(CO)_3Cl_2(THF)]$ has been reported.[24] We used computational DFT methods to estimate the energetics of this kind of solvent-assisted cleavage in the presence of methanol (see Scheme 2), ethanol (−30.8 kJ/mol), THF (−19.4 kJ/mol) and acetonitrile (−13.8 kJ/mol). The results showed that the reaction is energetically favorable in all the cases. However, it seems to be more favorable for alcohols than for THF or acetonitrile. Both THF and acetonitrile are more strongly coordinating ligands compared with alcohols, and this is an advantage in the case of alcohols because they can be replaced with other ligands more easily and thus are readily available for further reactions. Acetonitrile derivative requires refluxing conditions while the alcohol derivative does not require heating in order to react. The THF intermediate is in our case inconvenient since none of the selected ligands are very soluble in this solvent. In contrast, when alcohols were used the reactions were performed at room temperature and solubility of both the ruthenium dimer $[Ru(CO)_3Cl_2]_2$ and ligands was high.

Based on spectroscopic evidence, it has been suggested that $[Ru(CH_3CN)\ (CO)_3Cl_2)]$ is formed when $[Ru(CO)_3Cl_2]_2$ is heated under reflux in acetonitrile.[25] We were also able to isolate the product and verify the structure of the acetonitrile-containing tricarbonyl dichloro ruthenium compound by X-ray crystallography (see supplementary CIF information). In most cases the coordinating solvents tend to lead to symmetrical cleavage of the dimer and formation of a solvent derivative. The solvent can then be replaced relatively easily with various other monodentate ligands, including aromatic nitrogen ligands like pyrazine and pyridine. The structures of these complexes have been confirmed here by single-crystal X-ray crystallography (Figs 1 and 2).

Reactions with chelating ligands in alcoholic media

In general, the reaction between the ruthenium dimer and the bidentate chelating ligands [1,10′-phenanthroline $(N–N)_1$, 2,9′-dimethyl-1,10′-phenanthroline $(N–N)_2$, 4,7′-dimethyl-1,10′-phenanthroline $(N–N)_3$, 2,2′-bipyrimidine $(N–N)_4$ and 2,2′-bipyridine $(N–N)_5$] yielded products of the general

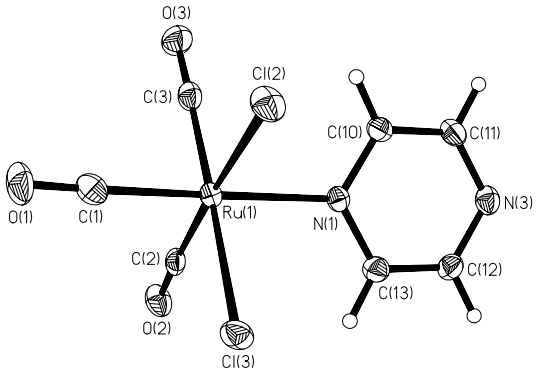

Figure 1. Thermal ellipsoids view of complex $[Ru(pz)(CO)_3Cl_2]$ (**22**) with atomic numbering scheme. Thermal ellipsoids are drawn with 50% probability. Selected bond lengths (Å) and angles (deg): Ru(1)–C(3), 1.900(2); Ru(1)–C(2), 1.918(2); Ru(1)–C(1), 1.934(3); Ru(1)–N(1), 2.145(2); Ru(1)–Cl(2), 2.3937(6); Ru(1)–Cl(3), 2.3986(6); C(1)–Ru(1)–N(1), 173.21(8); C(3)–Ru(1)–Cl(3), 178.63(7); C(2)–Ru(1)–Cl(2), 176.93(6).

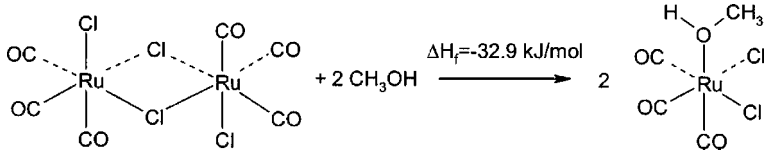

Scheme 2. Coordination of solvent and simultaneous cleavage of the ruthenium dimer by methanol.

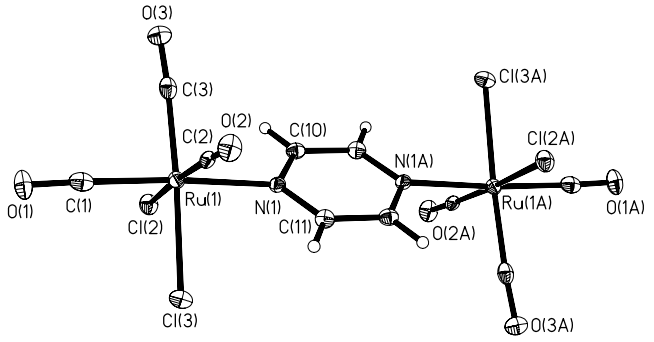

Figure 2. Thermal ellipsoids view of complex $[Ru(CO)_3Cl_2]_2(pz)$ (**23**) with atomic numbering scheme. Thermal ellipsoids are drawn with 50% probability. Selected bond lengths (Å) and angles (deg): C(1)–Ru(1), 1.915(3); C(2)–Ru(1), 1.923(3); C(3)–Ru(1), 1.906(3); N(1)–Ru(1), 2.144(2); Cl(2)–Ru(1), 2.4038(7); Cl(3)–Ru(1), 2.3918(7); C(3)–Ru(1)–Cl(3), 176.81(9); C(1)–Ru(1)–N(1), 176.27(10); C(2)–Ru(1)–Cl(2), 176.42(9).

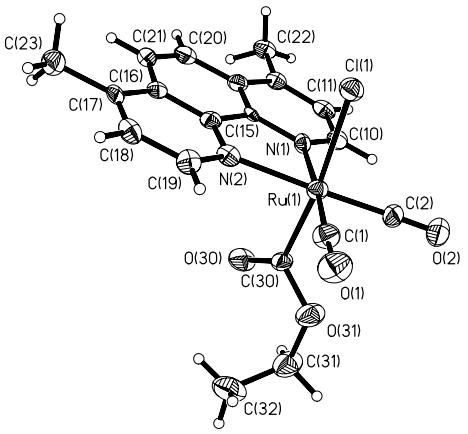

Figure 3. Thermal ellipsoids view of complex [Ru(4,7′-dimethyl -1,10′-phen)$(CO)_2Cl(COOCH_2CH_3)$] (**4**) with atomic numbering scheme. Thermal ellipsoids are drawn with 50% probability. Selected bond lengths (Å) and angles (deg): Ru(1)–C(1), 1.868(3); Ru(1)–C(2), 1.868(3); Ru(1)–C(30), 2.043(3); Ru(1)–N(2), 2.177(2); Ru(1)–N(1), 2.179(2); Ru(1)–Cl(1), 2.5144(7); C(30)–O(30), 1.193(3); C(30)–O(31), 1.347(3); O(31)–C(31), 1.448(4); C(1)–Ru(1)–C(2), 81.26(11); N(2)–Ru(1)–N(1), 77.72(7); C(30)–Ru(1)–Cl(1), 175.38(7); O(30)–C(30)–O(31), 120.2(3).

formula: [Ru(N–N)$(CO)_3$Cl(COOR)], R = CH_3 or CH_3CH_2, see for example Fig. 3.

The presence of the alkoxy carbonyl fragment is somewhat unexpected since formation of this kind of unit requires the presence of a suitable source of alkoxy ions that will act as nucleophiles able to attack one of the carbonyl carbons of the complex. The formation of this type of alkoxy carbonyl products is interesting since most of the reported metal alkoxy carbonyl complexes have been obtained from alkoxylation reactions of clusters in alkaline media.[26–28] In the case of ruthenium, alkoxy carbonyls have mostly been obtained from complexes that also undergo alkoxylation by strong bases such as sodium methoxide.[29–31]

In our case the alkoxy carbonyl fragments is formed at room temperature when the aromatic nitrogen ligand acts as a base, deprotonating the alcohol and generating alkoxy ions that are able to attack. The acidic behavior of alcohols has been computationally and experimentally studied,[32–34] and it has been suggested that they can behave as weak acids under appropriate conditions. On the other hand, the basicity of simple and aromatic amines has been established and a number of publications discussing the topic can be found in the literature.[35–37] Thus, the published work settles the grounds for our study. In our case the combination of the acidic behavior of alcohols combined with the basic character of aromatic amines in solution provides a suitable environment for acid–base reactions to take place. To have some insight regarding the basicity of the selected amine ligands we calculated the proton affinity, which is related to the gas phase basicity. A trend was observed following the order: 1,10′-phenanthroline (−1072.4 kJ/mol) > 2, 2′-bipyridine (−1047.1 kJ/mol) > 2, 2′-bipyrimidine (−990 kJ/mol) suggesting that 1,10′-phenanthroline has the strongest basic character. Another possibility for the generation of the alkoxy ions is via metal assisted deprotonation. Under this concept the solvent intermediate M-OHR could deprotonate giving M-OR + H and then when the bipyridine ligand (in excess) is in the media the proton coordinates to one of the nitrogens, producing the protonated ligand. Once the bidentate ligand is coordinated to the metal, the released alkoxy ions would attack one of the carbonyls, producing the alkoxycarbonyl complex.

Alkoxycarbonyls are not rare, for example, in cluster chemistry, and several examples of bridging alkoxy carbonyls are present in the literature.[38,39] Considering that our reactions were performed in the absence of conventional strong bases, alkoxides, and at room temperature in dry solvents, it can be suggested that the ligands themselves act as bases in alcoholic media, promoting the generation of the alkoxide ions.

After the ruthenium alkoxy products were separated from the reaction solution, another product containing ionic $[Ru(CO)_3Cl_3]^-$ was precipitated. The first of these products was identified as ion pairs of the type $[Ru(CO)_3Cl_3]^-[Ru(N–N)(CO)_3Cl]^+$ (complexes **7**–**9** and **16**–**17**, see for example Fig. 4). The mixture of the ruthenium carbonyl units gives a distinct IR pattern. For example in the case of 2,2′-bpmd ligand ν(CO) signals were found at 2047, 2059, 2072, 2092, 2126 and 2145 cm^{-1} corresponding the 2,2′-bpmd ion pair $[Ru(CO)_3Cl_3]^-[Ru(2, 2'\text{-bpmd})(CO)_3Cl]^+$ (**17**) shown in Fig. 4.

The nature of these sub-products is also of interest since the formation of these ion pairs implies that the production of alkoxy product is limited and, after reaching a certain point it stops, giving room for the formation of other products. It is also worth noticing that these products were obtained

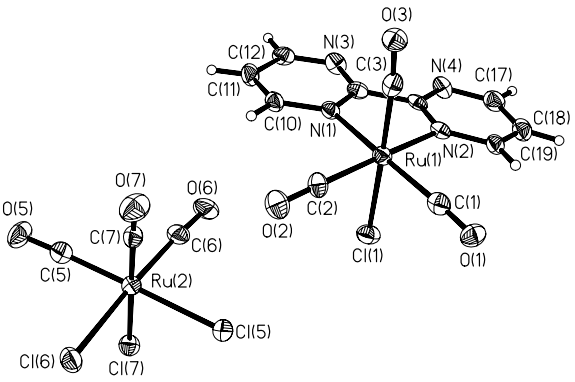

Figure 4. Thermal ellipsoid plot of $[Ru(CO)_3Cl_3]^-$ [Ru(2,2′-bpmd)$(CO)_3$Cl]$^+$(CH_2Cl_2) (**18**). The dichloromethane solvent has been omitted for clarity. Thermal ellipsoids are drawn with 50% probability. Selected bond lengths (Å) and angles (deg): Ru(1)–Cl(1), 2.389(2); Ru(1)–C(1), 1.932(9); Ru(1)–C(3),1.927(11); Ru(1)–C(2), 1.916(9); Ru(1)–N(1), 2.111 (7); Ru(1)–N(2), 2.093(7); C(1)–O(1), 1.124(10); C(2)–O(2), 1.126(10); C(3)–O(3), 1.131(11); Ru(2)–Cl(5), 2.406(2); Ru(2)–Cl(6), 2.406(2); Ru(2)–Cl(7), 2.429(2); Ru(2)–C(7), 1.885(11); Ru(2)–C(5), 1.885(10); Ru(2)–C(6), 1.910(9); C(5)–O(5), 1.131(11); C(6)–O(6), 1.117(11); C(7)–O(7), 1.147(11); C(2)–Ru(1)–C(1), 88.6(3); C(3)–Ru(1)–Cl(1), 177.8(3); N(2)–Ru(1)–N(1), 78.3(3); C(7)–Ru(2)–Cl(7), 177.8(3); Cl(6)–Ru(2)–Cl(5), 90.68(8); C(5)–Ru(2)–C(6) 94.3(4).

after the alkoxy product formed, suggesting that reduction in the metal–ligand ratio is key for obtaining the ion pairs exclusively. Thus, changes in the stoichiometry of the reaction allow control of the output. In order to study the influence of the stoichiometry, we performed the reaction varying the metal–ligand ratio. At a metal–ligand ratio of 1 : 2.5 the only product observed was the alkoxy complex. When the ratio was changed to 1 : 1 a mixture of both alkoxy product and ion pairs was observed. This mixture was also observed at a ratio 0.5 : 1. Finally, when the ratio was adjusted to 1 : 0.25, the only product obtained was the ion pairs. The mechanism for the formation of the alkoxy products and their corresponding ion pairs in alcohols is illustrated in Scheme 3.

From the same solution where the ion pairs $[Ru(CO)_3Cl_3]^-$ $[Ru(N–N)(CO)_3Cl]^+$ were separated, few crystals of another product precipitated. Again, it contained the $[Ru(CO)_3Cl_3]^-$ anion, but this time the counter cation was a protonated nitrogen ligand. For example, in the case of 2,9′-dimethyl-1,10′-phenanthroline the product was identified as $[Ru(CO)_3Cl_3]^-$[H(2, 9′-dimethyl-1,10′-phen)]$^+$ (**11**) (see for example Fig. 5). In these products the aromatic nitrogen ligand was not bonded to the ruthenium center, but protonated as a consequence of proton transfer from the solvent to the ligand. This provides further evidence of basic behavior of the nitrogen ligands in alcoholic media.

Although this type of product was observed only with 1,10′-phenanthroline, 2,9′ dimethyl-1,10′-phenanthroline and

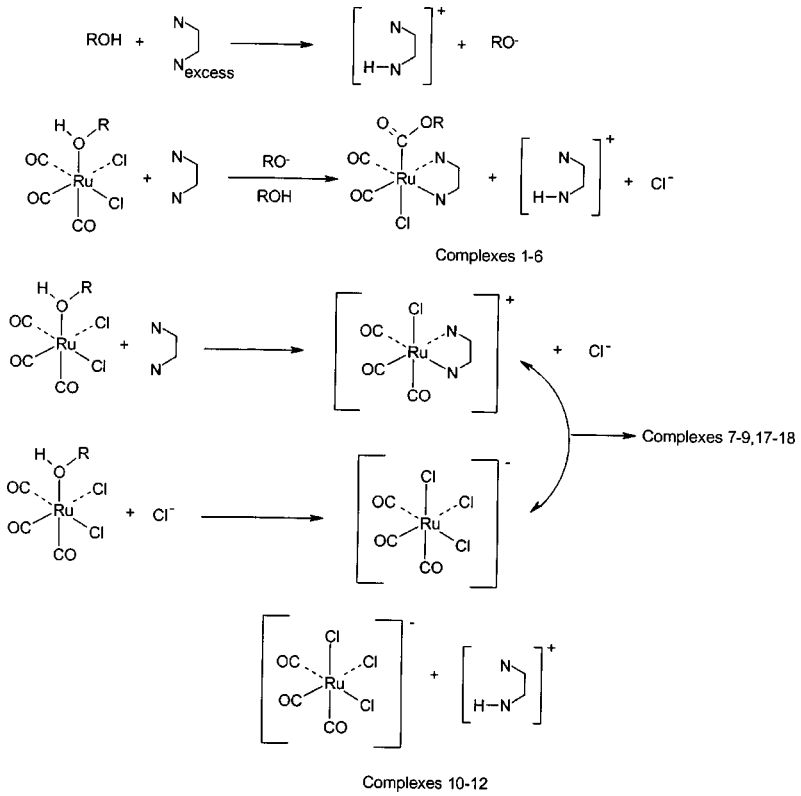

Scheme 3. Mechanism for the formation of alkoxy products and ion pairs in alcoholic media.

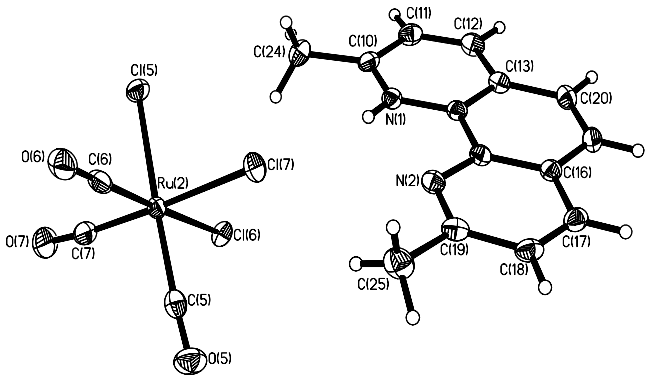

Figure 5. Thermal ellipsoid view of complex $[Ru(CO)_3Cl_3]^-$ $[H(2,9'\text{-dimethyl-}1,10'\text{-phen})]^+$ (**11**) with atomic numbering scheme. Thermal ellipsoids are drawn with 50% probability. Selected bond lengths (Å) and angles (deg): Ru(2)–Cl(5), 2.4079(5); Ru(2)–Cl(6), 2.4234(5); Ru(2)–Cl(7), 2.4227(5); Ru(2)–C(5), 1.911(2); Ru(2)–C(6), 1.889(2); Ru(2)–C(7), 1.908 (2); C(5)–O(5), 1.127(3); C(6)–O(6), 1.131(3); C(7)–O(7), 1.125(3); Cl(7)–Ru(2)–Cl(6), 91.27(2); C(5)–Ru(2)–Cl(5), 177.

4,7′-dimethyl-1,10′-phenanthroline, we can assume that the same occurs with the 2,2′-bipyrimidine and 2,2′-bipyridine since otherwise their behavior is similar.

When an excess of the nitrogen ligand, for example 2,9′-dimethyl-1,10′-phenanthroline, is used, the reaction proceeds directly to the formation of the alkoxy product $[Ru(2,9'\text{-dimethyl-}1,10'\text{-phen})(CO)_2Cl(COOCH_3)]$ (**5**). Once separated, the solution contains protons and chloride ions as a consequence of the formation of the alkoxy unit in the first product and the Ru–ligand ratio is reduced. This favors the formation of the ion pair $[Ru(CO)_3Cl_3]^-$ $[Ru(2,9'\text{-dimethyl-}1,10'\text{-phen})(CO)_3Cl]^+$ (**9**). However, the solution also contains chloride ions as well as protonated nitrogen ligands (see Scheme 3). This means that, after separating the alkoxy product, the solution contains four ions: $[Ru(CO)_3Cl_3]^-$, $[Ru(2,9'\text{-dimethyl-}1,10'\text{-phen})(CO)_3Cl]^+$, Cl^- and $[H(2,9'\text{-dimethyl-}1,10'\text{-phen}]^+$. From this solution it is possible to obtain crystals of $[Ru(CO)_3Cl_3]^-[H(2,9'\text{-dimethyl-}1,10'\text{-phen}]^+$; (**11**) however the ion pair $[Ru(CO)_3Cl_3]^-$ $[Ru(N–N)_3(CO)_3Cl]^+$ (**9**) is the preferred crystalline product and precipitates in good yields, in contrast to the ion pair with protonated nitrogen ligand. Evidence of the presence of chloride ions in solution was obtained by adding a few drops of a silver nitrate solution. The typical white precipitate of silver chloride was observed clearly.

Reactions with monodentate and bridging ligands in alcoholic media

It has been reported that in dichloromethane the reaction between pyrazine and the ruthenium dimer leads to monomeric $[Ru(pz)(CO)_3Cl_2]$ (**22**).[23] The same type of product is obtained when the dimer reacts with pyridine in dichloromethane.[25] The obvious difference between the

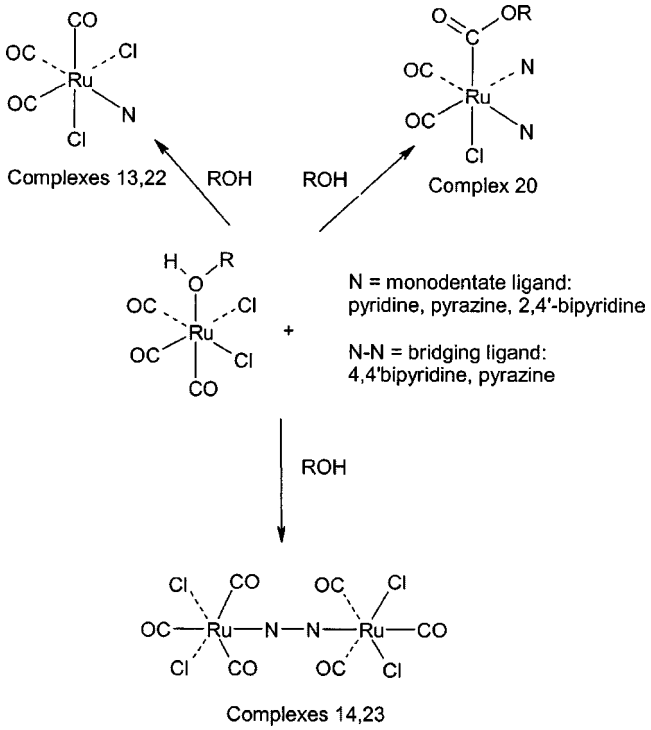

Scheme 4. Mono and bidentate complexes generated in reaction with mono and bridging ligands.

reactions of this type compared with the alcohol reactions is that the reaction pathway does not include direct participation of the solvent. The reaction of $[Ru(CO)_3Cl_2]_2$ with non-chelating ligands pyrazine (N_9), pyridine (N_8) 2,4′-bipyridine (N_7) or 4,4′-bipyridine (N_6) in alcoholic media can again involve the solvent. With pyrazine the product can contain either terminal nitrogen ligand (complex with one coordinated and one dangling nitrogen) or a bridging ligand. In the case of 4,4′-bipyridine only the bridged complex was observed. 2,4′-Bipyridine clearly favors the terminal nitrogen form with no evidence of bidentate bonding. Furthermore, in alcohols formation of alkoxycarbonyl compound was found again in the case of pyridine. So far, no alkoxy carbonyls were found with pyrazine. This may be due to lower basicity of pyrazine (Table 4). The reactions with monodentate and bridging ligands are summarized in the Scheme 4.

Dry reactions

The complex behavior of the chelating ligands in solution showed that these ligands are highly reactive. Therefore, we studied their reactivity in 'dry' solvent-free conditions. Thus, we performed the reactions in the absence of solvent simply by mixing $[Ru(CO)_3Cl_2]_2$ with the solid ligands in a mortar. Ruthenium complexes were obtained with the following ligands: 1,10′-phenanthroline $(N–N)_1$, 4,7′-dimethyl-1,10′-phenanthroline $(N–N)_2$, 2,9′-dimethyl-1,10′-phenanthroline $(N–N)_3$ and 2,2′-bipyrimidine $(N–N)_4$. The products were identified as the $[Ru(CO)_3Cl_3][Ru(N–N)(CO)_3Cl]$ ion pair

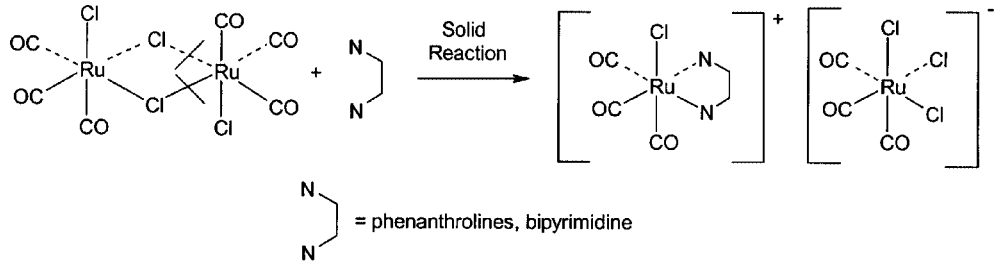

Scheme 5. Complexes obtained in the dry reactions.

described above (see Scheme 3). IR signals and elemental analysis of these products matched with the data already obtained for the same ion pairs obtained in solution (complexes **7–9, 17–18**). This confirms that the same product can be obtained with or without solvent. A general description of these reactions is illustrated in Scheme 5. Similar ion pairs have been obtained typically from cluster fragmentation.[40,41] To our knowledge, only one other example of asymmetric cleavage of the $[Ru(CO)_3Cl_2]_2$ with ion pair as the unique product has been reported. Reaction of $C_5H_5(Me_3Si)$ with $[Ru(CO)_3Cl_2]_2$ leads to an ion pair of $[Ru(CO)_3C_5H_5]^+[Ru(CO)_3Cl_3]^-$.[42] However, in this case the cyclopentadienyl ligand replaces both chlorides to give a tricarbonyl–Cp complex, whereas in our case just one chloride is replaced.

Energetics of the reactions

The formation of the ruthenium pyrazine, pyridine, and polypyridine complexes was further studied by computational DFT methods. This work was divided into two main categories: the reactions that produce alkoxy carbonyl products and the ones which do not involve alkoxycarbonyls. Because the reaction pathways are different, the calculated energies were compared only within each group but not between the groups. The goal was to find the most favorable reactions within both reaction pathways. In general, the use of chelating ligands, such as phenanthrolines and bipyrimidine, falls into the group of alkoxycarbonyl reactions and the use of non-chelating ligands mainly into the group of non-alkoxycarbonyl reactions. Computational results for the formation enthalpies are summarized in Table 2. All calculations assume gas phase, and the purpose of such calculations was to investigate how favorable these reactions were thermodynamically.

Chelating ligands

The model applied for the chelating bidentate nitrogen ligands in alcohol solutions is presented in equation (1):

$$[Ru(CO)_3Cl_2]_2 + 2\,(N{-}N) + 2\,ROH \longrightarrow 2[Ru(N{-}N)(CO)_2Cl(COOR)] + 2\,HCl \quad (1)$$

$(N{-}N) = (N{-}N)_1, (N{-}N)_2, (N{-}N)_3, (N{-}N)_4;$

$R = CH_3,$ or CH_2CH_3

Small steric and electronic effects explain the differences in behavior of different methyl substituted phenanthroline complexes compared with the non-substituted 1,10′-phenanthroline compound [Ru(1,10′-phen)$(CO)_2$Cl(COOR)] (**1**). In the case of 2,9′-dimethyl-1,10′-phenanthroline $(N{-}N)_3$, the methyl groups are located adjacent to the linking nitrogen, introducing steric stress. As a consequence, the formation enthalpy is increased in comparison with the 1,10′-phenanthroline complex. In 4,7′-dimethyl-1,10′-phenanthroline $(N{-}N)_2$ the methyl groups are far enough from the nitrogens not to induce any steric effects. Instead, the electronic effects become dominating since the methyl groups can effectively donate charge to the aromatic ring system and therefore to the binding nitrogens, increasing their reactivity. The enthalpy obtained with bipyrimidine is very close to those found in phenanthroline systems, suggesting that it behaves in essentially the same way as the phenanthrolines.

Previously, we studied the formation of [Ru(bpy)$(CO)_2$ Cl$(COOCH_3CH_2OH)$]. The formation enthalpy of −65 kJ/mol[21] for this ruthenium 2,2′-bipyridine complex is clearly less favorable than in the case of phenanthrolines or bipyrimidine. This is due to the rearrangement of the nitrogens in the bipyridine ring system. In free phenanthrolines and in bipyrimidine, the coordinating nitrogens are always in *cis* configuration while in the case of free 2,2′-bipyridine the actual configuration of the nitrogens is *trans*. Thus, in order to chelate, 2,2′-bipyridine has to undergo configuration change from *trans* to *cis*.[43] Therefore, it is expected that 2,2′-bipyridine initially attacks the metal center as a monodentated ligand. After coordination of one nitrogen the configuration is changed from *trans* to *cis*, allowing the second nitrogen to be attached to the metal center (see Scheme 6). Such rearrangement is not possible in the case of phenanthrolines because the ligand is rigid. In the case of bipyrimidine two of the nitrogens are always

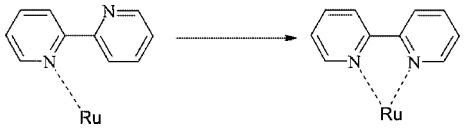

Scheme 6. Rearrangement from *trans* to *cis* in 2,2′-bipyridine.

cis. Thus, in the event of rearrangement of the bipyrimidine ligand, the final configuration would be identical with the initial configuration.

The effect of the rearrangement energy can also be seen when reaction of 2,2′-bipyridine is compared with the corresponding reactions with excess of pyridine. The product in pyridine reaction is bis(pyridine) $[Ru(py)_2(CO)_2Cl(COOCH_2CH_3)]$ (**20**), analogous to the 2,2′-bipyridine complex. The reaction enthalpy for pyridine reaction is again much more favorable (−150 kJ/mol) than in the case of 2,2′-bipyridine. It should be noted that, even though pyridine is a non-chelating ligand, the product is an alkoxy carbonyl as well. Thus, both products are formed following the same mechanism.

Non-chelating ligands

The computational model applied for the reactions of monodentate and bridging ligands is presented in equation (2):

$$[Ru(CO)_3Cl_2]_2 + 2\,N \longrightarrow 2\,[Ru(N)(CO)_3Cl_2] \qquad (2)$$

$$N = N_6,\ N_7,\ N_8 \text{ and } N_9$$

The reaction enthalpies vary from −41 to −92 kJ/mol. The most favorable values are obtained with 2,4′-bipyridine and with pyridine. With ligands that are able to form linear bridges, the enthalpy values are mostly smaller. Experimentally, the main product in the reaction between pyrazine and $[Ru(CO)_3Cl_2]_2$ was monomeric $[Ru(pz)(CO)_3Cl_2]$ (**22**). The dimeric $[Ru(CO)_3Cl_2]_2(pz)$ (**23**) was formed only as a minor product. This is also in agreement with the computational results: the formation of $[Ru(pz)(CO)_3Cl_2]$ (**22**) is energetically more favorable. The other linear bridging ligand, 4,4′-bipyridine, behaves differently. In this case the major product was found to be 4,4′-bipyridyl bridged $[Ru(CO)_3Cl_2]_2$(4,4′-bpy) (**14**). In fact, the corresponding monomer $[Ru(4,4'\text{-bpy})(CO)_3Cl_2]$ was not observed at all.

Reactivity studies

All the complexes prepared were used as catalysts for the hydroformylation of 1-hexene in order to study their reactivity. The activity results were then correlated to the role of the ligand by estimating the reactivity of the ligands themselves and the effect of coordination over the catalytic behavior. For this we calculated proton affinities, bite angles and association energies and finally proposed a catalytic cycle for the hydroformylation of 1-hexene.

Catalysis

Typically ruthenium carbonyl nitrogen-containing catalysts are known to be moderately active for hydroformylation,[44,45] and those which display high activities generally work under high pressures and temperatures.[46] The results observed for the hydroformylation of 1-hexene are presented in Table 3.

The catalytic studies revealed a group of catalysts that display modest conversions and selectivities at low values of temperature and pressure. Catalysts can be classified into three groups in terms of activities, group 1 including complexes containing bidentate ligands such as phenanthrolines and 2,2′-bipyridines, group 2 involving complexes with monodentate ligands of the polypyridine-type like 2,4′-bipyridine, 4,4′-bipyridine and pyrazine, and group 3 restricted to pyridine. Catalysts from group 1 show no activity under the reaction conditions with the exception of 2,2′-bipyridines, which favor the production of alcohols to a small extent. The lack of reactivity of the phenanthroline catalysts under catalytic conditions is associated with the stability introduced by the chelate ring. Once the chelate is formed, the complex is unable to accommodate another ligand. Breakdown of the chelate to create a vacancy for coordination is unlikely because the chelate ring is a highly stable system. In group 2, monomeric and dimeric versions of ruthenium pyrazine, and monodentate 2,4′- and 4,4′-bipyridines ruthenium complexes, show good activity towards the hydroformylation of 1-hexene. At this point the presence of a ligand in the catalyst structure has a negative effect since the ruthenium dimer itself is able to catalyze the reaction more effectively than the catalysts in groups 1 and 2. However, the results obtained while using monosubstituted pyridine-containing catalysts suggests that, in this case, the presence of the ligand enhances the activity and selectivity towards production of aldehydes. In all the cases small increase on temperature (10 °C) results in the total conversion of 1-hexene to the corresponding alcohols with the total absence of the typical side reactions such as isomerization and hydrogenation of the substrate (see Fig. 6). According to our results, the bridged complexes seem to favor the production of alcohols while monomers produce mainly aldehydes; in both cases the main product is the terminal alcohol or aldehyde.

There seems to be a relationship between rigidity of the ligands and activity; thus highly restricted structures as phenanthrolines show no activity, but when the degree of restriction is reduced activity begins to rise (see Fig. 1). Hence, bidentate bipyridine is active but yet not as much as monodentate bipyridine, pyridine or pyrazine. In contrast to the other compounds, the group of phenanthroline-containing catalysts shows no conversion even at high temperatures and pressures. Such behavior suggests that these compounds are more stable and unlikely to react. NMR and FTIR analysis of the solid recovered after catalysis reaction show no decomposition of the catalysts, confirming that neither the organic ligands nor carbonyls are lost during the catalysis. In other words, the catalyst is regenerated after the products are formed. In light of the evidence of regeneration, we propose here a plausible catalytic cycle that includes pathways for both the hydroformylation of 1-hexene and hydrogenation of the aldehydes produced (Schemes 7 and 8).

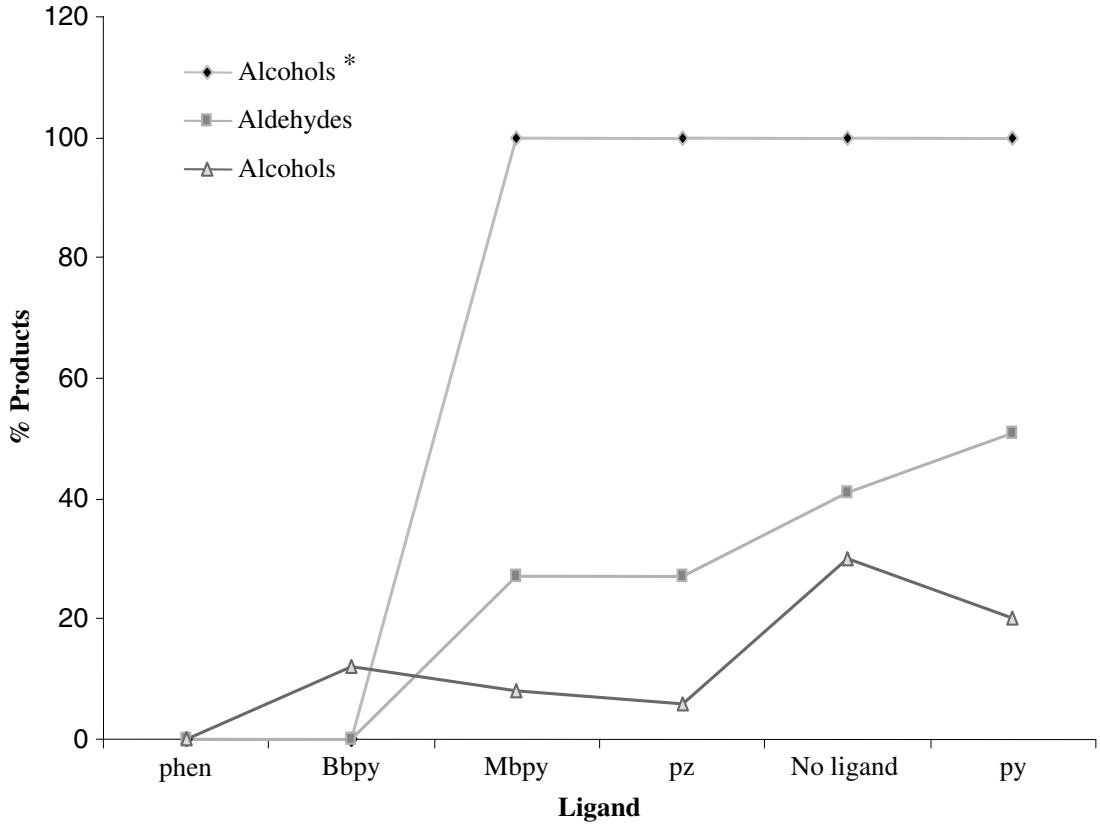

Figure 6. Ligand effect on the selectivity of the hydroformylation reaction; phen = phenanthrolines; Bbpy = bidentate bipyridine; Mbpy = monodentate bipyridine; pz = pyrazine; py = pyridine; alcohols* = alcohols obtained at 130 °C.

Reactivity and stability studies

In order to study the reactivity of the ligands we have calculated single proton affinities for the monodentate ligands and natural bite angle for bidentate ligands, to try to find a general trend regarding the behavior of these organic compounds. The results are displayed in Table 4.

Considering proton affinity of the monodentate ligands, a clear trend can be found: bipyridine > pyridine > pyrazine. This trend is also consistent with the catalytic activity of the ruthenium complexes (see Table 3). This suggests that the ligand plays a role in determining the stability in the coordinated complexes. Thus, to study further the actual interaction metal–ligand we calculate the complexation energy by applying the following model [equation (3)]. This model only considers a ruthenium atom and the coordination of one ligand. The goal is to estimate whether the formation of a chelate is energetically more favorable than the coordination of a monodentate ligand.

$$\mathrm{Ru} + \mathrm{L} \longrightarrow \mathrm{Ru} - \mathrm{L} \qquad (3)$$

$$\mathrm{L} = \text{pyridine, pyrazine, 2, 2′-bipyridine, 1, 10′-phenanthroline}$$

The energy value is an indication of the degree of stability of the coordinated complexes. Thus, the more favored the association, the more stable the complex is, and consequently the less reactive. Under these terms the association energies are consistent with the experimental data, and activity studies fully support the same trend, as indicated by Fig. 7.

The complexation energies for the bidentate ligands are considerably higher than those for monodentate ligands, suggesting that the interaction metal ligand is stronger and the chelating effect is appreciable and moreover theoretically measurable.

The calculation of the natural bite angles was made on the basis of the original concept developed by Casey and co-workers.[48] Natural bite angles for all bidentate ligands are between 83.02 and 81.77°. Although the variations in bite angles are too small to draw any meaningful conclusions, they still follow the reactivity pattern phenanthrolines < bidentate bipyridines < pyrazine < pyridine. The small variations in bite angles indicate that their influence over the catalytic activity is insignificant. For the bite angle to have an effect over activity and selectivity, the values must be around 100–120°,[49] lower values of bite angle imply that the geometry of the biting ligand cannot stabilize a particular configuration in the active intermediate;[50] therefore it is unable to improve activity or selectivity.

The structural rigidity of the ligands follows the order: phenanthrolines > bipyridines > pyridine ≈ pyrazine. This

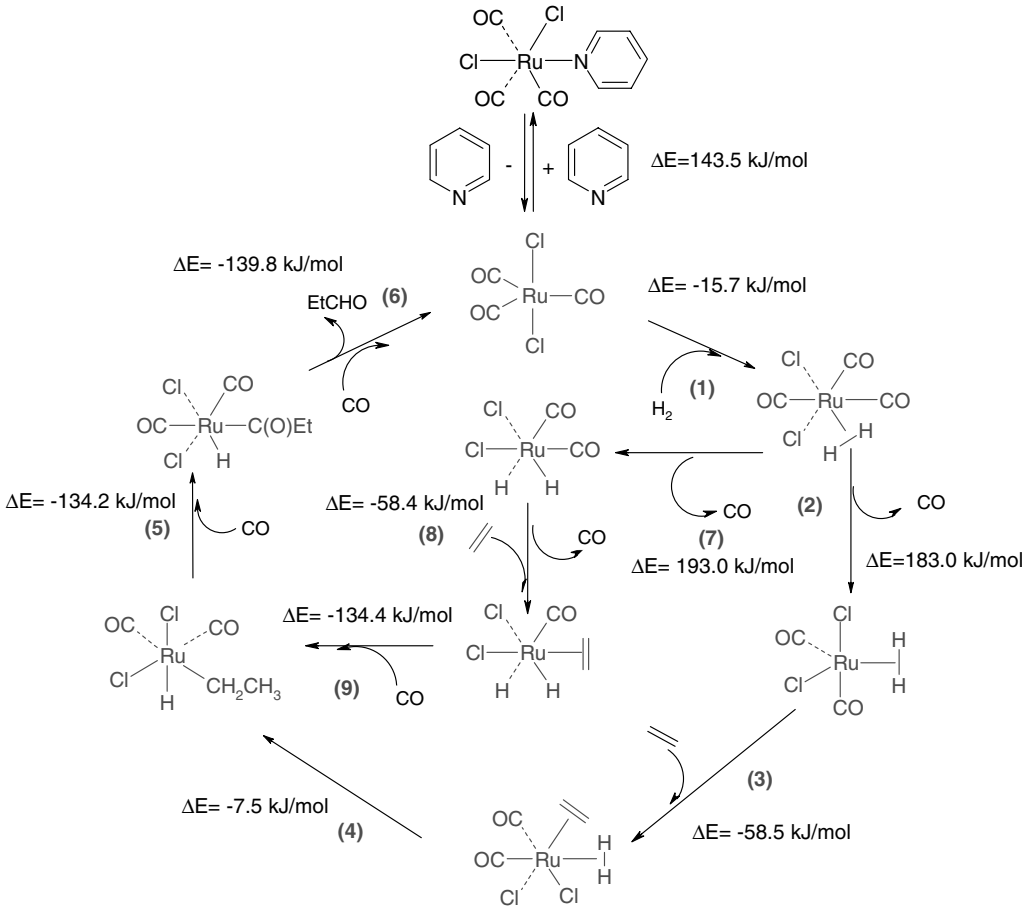

Scheme 7. Catalytic routes for the hydroformylation of ethylene by $[Ru(py)(CO)_3Cl_2]$.

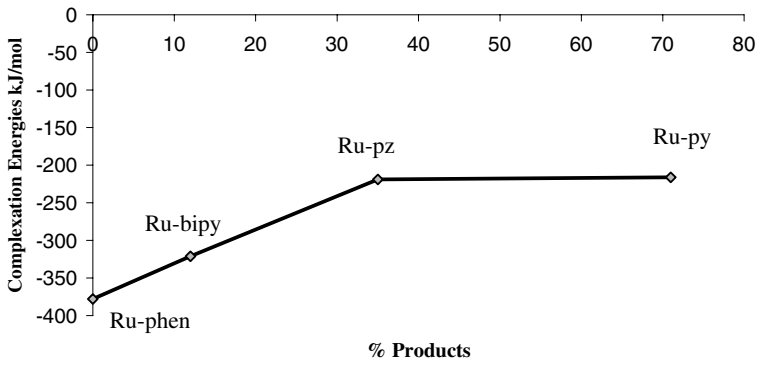

Figure 7. Correlation of activity–stability for the coordinated complexes.

is of particular importance because the structure of the ligand has an important influence on the coordination mode and consequently in the cleavage mode of the ruthenium dimer. Thus, 2,2′- and 4,4′-bipyridines typically behave as bidentate ligands, displaying low activities by coordinating to the metal through both nitrogens. In contrast, 2,4′-bipyridine behaves more like a typical monodentate ligand. Pyrazine, on the other hand, can behave as a monodentate ligand (Fig. 2) when forming mono-substituted complexes or as a bidentate ligand when the corresponding bridged complex forms (Fig. 2).

Catalytic cycles

The complex that showed the highest activity was the mononuclear $[Ru(py)(CO)_3Cl_2]$ (**21**). In light of the evidence of regeneration, we propose a plausible catalytic cycle that includes pathways for both hydroformylation of 1-hexene

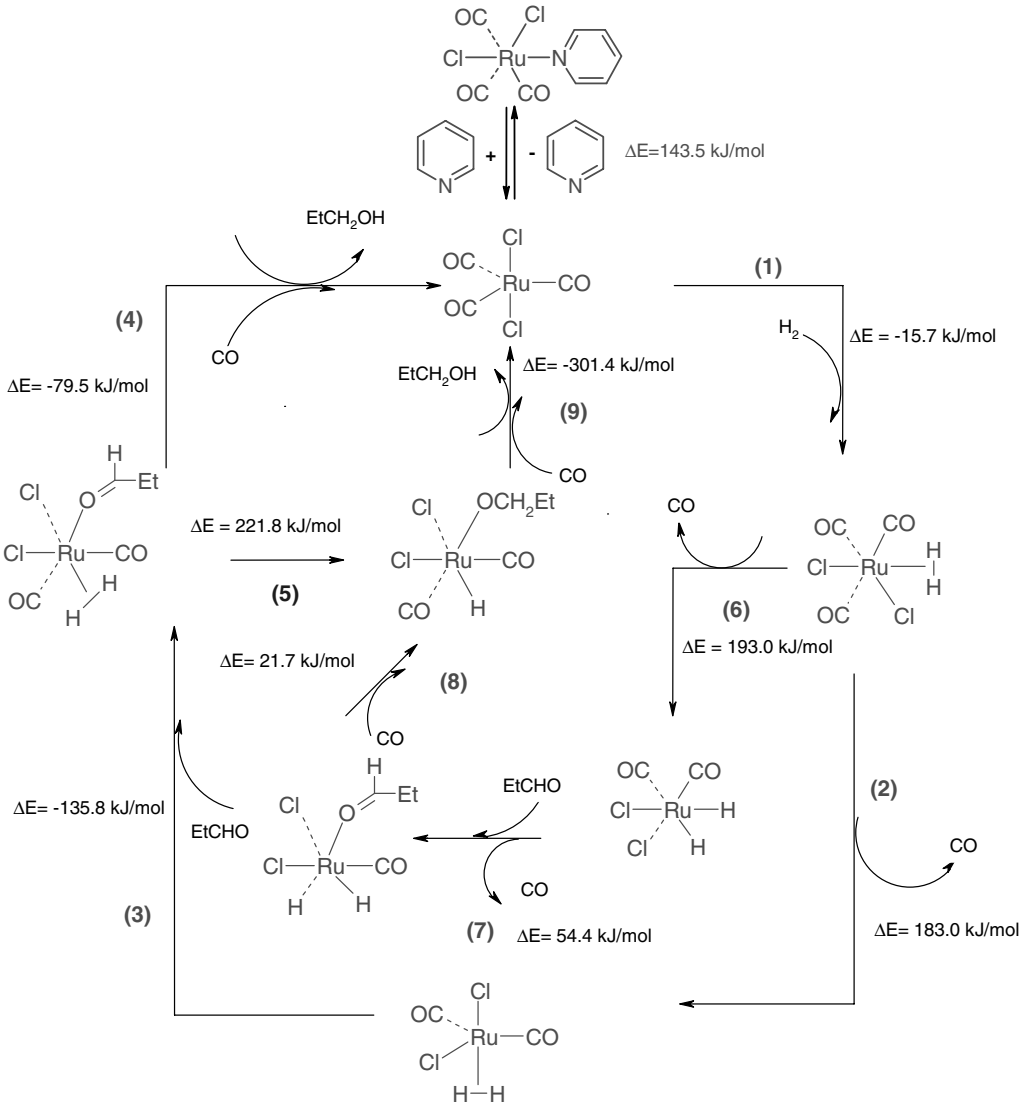

Scheme 8. Catalytic routes for the hydrogenation of propanal by $[Ru(py)CO)_3Cl_2]$.

and hydrogenation of the aldehydes produced (Schemes 7 and 8)

The cycles were modeled in gas phase using ethylene as the alkene in order to restrict the energy contributions due to rotation of the saturated tail in 1-hexene. In both cycles an initiation step involving the loss of the pyridine ligand, in order to generate the vacancy is proposed based on the fact that the ruthenium dimer catalyzes effectively the reaction when no ligand is present. Experimental evidence of the loss of the pyridine ligand was observed when a ligand exchange reaction was performed. The complex exchanges pyridine for triphenyl phosphine under catalytic conditions, as indicated by NMR and IR spectroscopy.

In the hydroformylation routes two possibilities are considered. The first involves dihydrogen intermediates (steps 1–6) and the other considers dihydride species (steps 1, 7–9 and 5–6). In both cases, a pentacoordinated ruthenium complex proceeds to take up hydrogen and then to lose a carbonyl, generating a vacancy where the alkene coordinate is, leading to the addition of hydrogen to the double bond either via intramolecular hydrogen transfer from a dihydrogen intermediate[51,52] or from a dihydride complex via oxidative addition. Carbonyl insertion is the next step, followed by the generation of the aldehyde unit.

In the hydrogenation routes three possibilities are considered. The first (steps 1–4) consider dihydrogen intermediates and simultaneous hydrogen transfer mechanism.[53] The second route (steps 1 and 6–9) considers formation of dihydride intermediates before hydrogenation of the aldehyde. Finally the third pathway (steps 1–3, 5 and 9) assumes a stepwise hydrogen transfer mechanism.[51,52] In all cases, the same tricarbonyl dichloride ruthenium complex coordinates hydrogen in the form of a dihydrogen unit as the initial step. In the next step another carbonyl is released and, depending on the

mechanism under consideration, a dihydride forms (step 6) or a vacancy for coordination of the aldehyde is created (step 2). The next step involves coordination of the aldehyde unit: step 3 in dihydrogen cycle and step 7 in dihydride cycle. The final step of hydrogenation can occur via simultaneous hydrogen transfer (step 4) as suggested by Poliakoff[53]. It can also proceed via stepwise hydrogen transfer[51] (step 5) or, finally, via dihydride (step 8), releasing the corresponding alcohol and regenerating the initial active complex. Experimental results concerning activity show that hydrogenation of the aldehydes is reduced when pyridine is present compared with the case in which no ligand is coordinated to ruthenium, suggesting a possible competition between the aldehyde unit and the pyridine ligand for coordination to the ruthenium center.

According to our model the initiation step requires the loss of the nitrogen- containing ligand. Under these conditions, activities related to all catalysts of pyridine, pyrazine and monodentate bipyridine should be similar since the ligand is the first to leave the ruthenium complex and none of the proposed active species includes them. However, in the case of pyrazine and monodentate bipyridines they are able to form stable dimers that reduce the activity considerably. The calculated energies for the loss of pyrazine, pyridine and monodentate bipyridine are as follows: pyrazines (131.3 kJ/mol) <pyridine (143.5 kJ/mol) <2, 4′-bipyridine (151.0 kJ/mol). The energy values indicates that pyrazine is easier to release from the ruthenium carbonyl complex, but the fact that pyrazine also dimerizes even easier opens up the possibility that, at the moment of initiation, dimers form reducing the amount of monopyrazine complex and consequently the activity. The same approximation applies to the case of monodentate bipyridines. On the other hand, pyridine is not able to dimerize for which reason reduction of activity is not observed. Once these dimers are formed, the energy required to break them is considerably higher. Thus, for the Ru-4,4′-bipyridine-Ru dimer, 277.1 kJ/mol are necessary to dissociate the dimer into two monomers and for the Ru-pz-Ru 250 kJ/mol. These values are consistent with the activity behavior observed for these species. Changes in the pressure conditions led to the domination of one cycle over the other. Thus, high pressures favor the hydrogenation of the aldehyde and the main products consists of alcohols, while at low pressures the dominant cycle is the one in which aldehydes are the main product.

The generally accepted mechanism for the rhodium-catalyzed hydroformylation of alkenes, by Heck and Breslow, implies a catalytic precursor that contains hydrides and activates through release of one phosphine ligand. In ruthenium-catalyzed hydroformylation most of the reported mechanisms are for phosphine-containing precursors as well.[54,55] In most of the cases the activation mechanism is analogous to that proposed for rhodium. On the other hand, catalytic precursors that do not contain phosphines operate for, example, through changes in the oxidation state of the metal, promoting activation.[56,57] In our case, the precursor does not contain bulky ligands that can be released by operation of steric effects, and the oxidation state of the complex remains constant during the cycle. Interestingly, our calculations suggested initially that activation was highly favored by the release of a carbonyl ligand (120 kJ/mol). However, no evidence of CO in the gas phase was observed. Furthermore, the fact that the activities observed with $[Ru(py)(CO)_3Cl_2]$ (**21**) catalyst are comparable to the ones observed when $[Ru(CO)_3Cl_2]_2$ was used in the absence of any ligands suggests that effectively the ligand is lost. If the pyridine ligand played a significant role in the catalyst, it would be reflected in the activities and this was not observed. Also, the results from the exchange reaction support the loss of pyridine rather than CO. The complex exchanges pyridine for triphenyl phosphine. Although the release of CO seems to be the less demanding pathway for activation, when the rest of the steps in the cycle were calculated for a pyridine-containing catalyst, the energies were considerably higher and most of the steps were unfavorable. It is interesting then to see that a small and relatively strongly coordinated ligand such as pyridine can de-coordinate so readily.

CONCLUSIONS

Direct participation of the alcohol solvent and the formation of alkoxy carbonyl products in the reaction between $[Ru(CO)_3Cl_2]_2$ and polypyridines was observed in the cases of phenanthrolines, bipyridines and pyridine. Such behavior suggests that these ligands act as bases in alcoholic media. The acid–base interaction between the nitrogen ligand and alcohol solvent generates the alkoxy ions in the solution. The possibility of using alcohols as a source for alkoxy ions provides an effective synthetic route to various alkoxy carbonyl complexes. The nucleophilic attack of the alkoxy ions to a carbonyl carbon attached to a metal center leads to formation of the final alkoxycarbonyl unit.

The bidentate chelating phenanthrolines are highly reactive and able to coordinate to ruthenium at room temperature and even in the absence of solvent. Unlike in alcohols, the 'dry' solvent-free reaction leads to asymmetric cleavage of $[Ru(CO)_3Cl_2]_2$, producing ionic $[Ru(CO)_3Cl_3]^-[Ru(N–N)(CO)_3Cl]^+$.

The interaction between the aromatic nitrogen ligand and the ruthenium center determines the reactivity of the new complexes. This effect can be clearly seen in the catalytic behavior of the products. When the interaction becomes weaker the activity increase follows the order: phenanthroline < bipyrimidine < chelated bipyridine < bridged bipyridine ≈ monodentate bipyridine ≈ pyrazine < pyridine. In each of the cases, addition of an aromatic nitrogen ligand decreases the catalytic activity compared with the bare ruthenium carbonyl catalyst. The systems with nitrogen-containing aromatic ligands of bidentate nature or with the ability to form bridges decrease the activity more drastically compared with the monodentate ligands.

The simple model employed to calculate complexation energies for the selected aromatic nitrogen ligand describes well the chelating effects and metal–ligand interactions. This approach proved useful to explain the factors behind the stability of the complexes and behavior of different ligands.

EXPERIMENTAL

FTIR measurements were performed on a Nicolet Magna 750 spectrometer. ^{1}H NMR of the metallic complexes was recorded on a Brucker Avance with a resonance frequency of 250 MHz. Elemental analyses were done on EA1110 CHNS-O equipment (CE Instruments) 1,10′-phenanthroline, 4,7′-dimethyl-1,10′-phenanthroline and 2,9′-dimethyl-1,10′-phenanthroline were used without further purification and were obtained from Aldrich. Pyrazine and pyridine were obtained from Fluka. All reactions were performed under nitrogen and the solvents were degassed as well prior to use. Crystals were obtained by recrystallization from a mixture 1 : 1 of hexane and dichloromethane.

General procedure for the synthesis of [Ru(N–N)(CO)$_2$Cl(COOR)] complexes

$(N–N)_1 = 1, 10'$-phenanthroline, $(N–N)_2 = 4, 7'$-dimethyl-1, 10′-phenanthroline, $(N–N)_3 = 2, 9'$-dimethyl-1,10′-phenanthroline; R = CH_3CH_2O, CH_3O. A 20 mg (0.039 mmol) aliquot of $[Ru(CO)_3Cl_2]_2$ was dissolved in 1.5 ml of ROH. A 30 mg (0.166 mmol) aliquote of $(N–N)_1$, 30 mg (0.144 mmol) of $(N–N)_2$ and 30 mg (0.144 mmol) of $(N–N)_3$, respectively were also dissolved in 1.5 ml of ROH; both solutions were stirred until dissolution and mixed. The combined solution was stirred overnight. A solid white precipitated was formed. The solid was washed with alcohol and dried under vacuum. Yields refer to the pure product.

*[Ru(N–N)$_1$(CO)$_2$Cl(COOCH$_3$)] (**1**)*

$(N–N)_1 = 1, 10'$-phenanthroline. Colorless crystals, ν(CO) = 2058, 1995, 1635 cm^{-1} in CH_2Cl_2, δ_H($CDCl_3$) 9.36d ($H_9^{9,8}J$ = 5 Hz), 8.58d ($H_7^{7,8}J$ = 4.8 Hz), 8.04 s(H_5), 7.93dd ($H_8^{8,9}J$ = 5 Hz) 3.388s(CH_3 in alkoxy group). δ_C($CDCl_3$) 198.57 ($COOCH_3$), 193.85(CO), 153.27(C_9), 147.09(C_{11}), 138.79(C_7), 131.44(C_6), 128.26(C_5), 126.23(C_8). Anal. calcd, N 6.49%, C 44.51%, H 2.57%. Found, N 6.56%, C 44.25%, H 2.56%. Yield = 89%.

*[Ru(N–N)$_1$(CO)$_2$Cl(COOCH$_2$CH$_3$)] (**2**)*

$(N–N)_1 = 1, 10'$-phenanthroline. Colorless crystals, ν(CO) = 2057, 1994, 1632 cm^{-1} in CH_2Cl_2, δ_H($CDCl_3$) 9.37dd ($H_9^{9,8}J$ = 6.3 Hz), 8.57dd ($H_7^{7,8}J$ = 4.8 Hz), 8.03s(H_5), 7.91dd ($H_8^{8,9}J$ = 6.3 Hz), 3.62q (CH_2 in alkoxy group J = 10.8 Hz), 1.025t (CH_3 in alkoxy group J = 7 Hz). δ_C($CDCl_3$) 198.69($COOCH_3$), 193.23(CO), 153.22(C_9), 147.07(C_{11}), 138.74(C_7), 131.38(C_6), 128.2(C_5), 126.21(C_8), 59.94 (CH_2 in alkoxy group), 15.23(CH_3 in alkoxy group). Anal. Calcd, N 6.28%, C 45.80%, H 2.94%. Found, N 6.37%, C 45.60%, H 2.95%. Yield = 87%.

*[Ru(N–N)$_2$(CO)$_2$Cl(COOCH$_3$)] (**3**)*

$(N–N)_2 = 4, 7'$-dimethyl-1,10′-phenanthroline. Colorless crystals, ν(CO) = 2055, 1992, 1637 cm^{-1} in CH_2Cl_2, δ_H($CDCl_3$) 9.20d ($H_9^{9,8}J$ = 2.5 Hz), 8.19s(H_5), 7.71dd ($H_8^{8,9}J$ = 2.5 Hz), 2.94s(4,7′-CH_3), 3.385s(CH_3 protons from alkoxy group). δ_C($CDCl_3$) 198.8($COOCH_3$) 194.3 (CO), 152.8(C_9) 148.9(C_7), 146.9(C_{11}), 130.9(C_6), 126.9(C_5), 124.3(C_8), 51.6(CH_3 in alkoxy group) 19.6(4,7′-CH_3). Anal. calcd, N 6.23%, C 47.01%, H 3.29%. Found, N 6.15%, C 46.7%, H 3.35%. Yield = 86%.

*[Ru(N–N)$_2$(CO)$_2$Cl(COOCH$_2$CH$_3$)] (**4**)*

$(N–N)_2 = 4, 7'$-dimethyl-1,10′-phenanthroline. Colorless crystals, ν(CO) = 2055, 1991, 1630 cm^{-1} in CH_2Cl_2, δ_H($CDCl_3$) 9.20d ($H_9^{9,8}J$ = 2.6 Hz), 8.14s(H_5), 7.70dd ($H_8^{8,9}J$ = 2.6 Hz), 3.83d (CH_2 from alkoxy group J = 10.5 Hz), 2.93s (4,7′-CH_3), 1.38t (CH_3 in alkoxy group J = 7.5 Hz). δ_C($CDCl_3$) 198.9($COOCH_3$), 193.7(CO), 152.7(C_9), 148.80(C_7), 146.9(C_{11}), 130.8(C_6), 126.8(C_5) 124.2(C_8), 59.82(CH_2 in alkoxy group) 19.643(4,7′-CH_3), 15.27(CH_2 in alkoxy group). Anal. calcd, N 5.91%, C 48.16%, H 3.62%. Found, N 6.03%, C 47.97%, H 3.66%. Yield = 84%.

*[Ru(N–N)$_3$(CO)$_2$Cl(COOCH$_3$)] (**5**)*

$(N–N)_3 = 2, 9'$-dimethyl-1,10′-phenanthroline. Colorless crystals, ν(CO) = 2055, 1989, 1640 cm^{-1} in CH_2Cl_2, δ_H($CDCl_3$) 8.36d ($H_7^{7,8}J$ = 4 Hz), 7.881s (H_5), 7.72d ($H_8^{8,7}J$ = 4 Hz), 3.37s (2,9′-CH_3), 3.40s(CH_3 in alkoxy group). δ_C($CDCl_3$) 198.3 ($COOCH_3$) 193.6 (CO), 163.6 (C_9), 148.4 (C_{11}), 139.1(C_7), 129.4(C_6), 127.0(C_5), 126.8(C_8), 51.8(CH_3 in alkoxy group), 30.4(2,9′-CH_3). Anal. calcd, N 6.09%, C 47.01%, H 3.29%. Found, N 6.14%, C 46.78%, H 3.41%. Yield = 82%.

*[Ru(N–N)$_3$(CO)$_2$Cl(COOCH$_2$CH$_3$)] (**6**)*

$(N–N)_3 = 2, 9'$-dimethyl-1,10′-phenanthroline. ν(CO) = 2054, 1988, 1632 cm^{-1} in CH_2Cl_2, δ_H($CDCl_3$) 8.36d ($H_7^{7,8}J$ = 4 Hz), 7.86s (H_5), 7.73d ($H_8^{8,7}J$ = 4 Hz), 3.82s (2,9′-CH_3), 3.42s(CH_2 in alkoxy group), 0.9t(CH_3 in alkoxy group) δ_C($CDCl_3$) 198.3 ($COOCH_3$) 192.8 (CO), 163.5 (C_9), 148.3 (C_{11}), 139.0(C_7), 129.3(C_6), 127.0(C_5), 126.9(C_8), 59.9(CH_2 in alkoxy group), 30.4(2,9′-CH_3), 15.2 (CH_3 in alkoxy group). Anal. calcd, N 6.09%, C 47.01%, H 3.29%. Found, N 6.14%, C 46.78%, H 3.41%. Yield = 82%.

General procedure for the synthesis of [Ru(CO)$_3$Cl$_3$]$^-$ [Ru(N–N)(CO)$_3$Cl]$^+$ complexes

These complexes were synthesized following the same procedure as for complexes **1**–**6**, but changing the metal–ligand ratio to 1 : 0.25. Yields are referred to the pure product. For the dry reactions a 1 : 0.5 metal–ligand ratio was used. The reactants were mixed in a mortar thoroughly and the mixture was allowed to react. After a period of 1 h a change in color from pale yellow to pink-red indicated reaction had taken place.

*[Ru(CO)$_3$Cl$_3$]$^-$ [Ru(N–N)$_1$(CO)$_3$Cl]$^+$ (**7**)*

$(N–N)_1 = 1, 10'$-phenanthroline, ν(CO) = 2050, 2075, 2093, 2125, 2145 cm^{-1} in CH_2Cl_2. δ_H($CDCl_3$) 9.36d ($H_9^{9,8}J$ = 4.5 Hz);

8.82d (H_7 $J = 4.25$ Hz); 8.174 s (H_5); 8.04dd ($H_8J = 4.5$ Hz). $\delta_C(CDCl_3)$ 187.3 (CO), 156.3 (C_9), 146.9 (C_{11}), 142.8 (C_7), 133.1(C_6), 129.6(C_5), 128.36(C_8). Anal. calcd, N 4.05%, C 31.23%, H 1.16%. Found, N 4.11%, C 31.27%, H 1.18%. Yield = 60%

*$[Ru(CO)_3Cl_3]^-$ $[Ru(N{-}N)_2(CO)_3Cl]^+$ (**8**)*

$(N{-}N)_2$ = 4, 7′-dimethyl-1,10′-phenanthroline, ν(CO) = 2048, 2065, 2086, 2095, 2117, 2145 cm^{-1} in CH_2Cl_2. $\delta_H(CDCl_3)$ 9.42d ($H_9{}^{9,8}J = 2, 6$ Hz) 8.28s (H_5) 8.03d ($H_8{}^{8,9}J = 2.5$ Hz) 2.91m (4,3 CH_3). Anal. calcd, N 4.06%, C 31.60%, H 1.98%. Found, N 4.08%, C 31.57%, H 1.88%. Yield = 48%

*$[Ru(CO)_3Cl_3]^-$ $[Ru(N{-}N)_3(CO)_3Cl]^+$ (**9**)*

$(N{-}N)_3$ = 2, 9′-dimethyl-1,10′-phenanthroline, ν(CO) = 2043, 2066, 2094, 2117, 2144 cm^{-1} in CH_2Cl_2. $\delta_H(CDCl_3)$ 8.62d ($H_8{}^{8,7}J = 4.25$ Hz) 8.03s (H_5) 7.91d ($H_7{}^{7,8}J = 4.25$ Hz) 3.38s (2,9′-CH_3) $\delta_C(CDCl_3)$ 186.2(CO), 160.4 (C_9), 128.3 (C_6), 141.4 (C_7), 137.2 (C_{11}), 127.3 (C_5) 125.2 (C_8) 19.8 (CH_3). Anal. calcd, N 4.06%, C 31.60%, H 1.98%. Found N 4.01%, C 31.62%, H 1.78%. Yield = 51%.

General procedure for the synthesis of $[Ru(CO)_3Cl_3]^-$ $[H(N{-}N)]^+$ complexes

These products were not obtained following a synthetic procedure, instead they crystallized in very low quantities from the solution remaining after separating the alkoxy complexes $[Ru(N{-}N)(CO)_2Cl(COOR)]$ and the ion pairs $[Ru(CO)_3Cl_3]^-$ $[Ru(N{-}N)(CO)_3Cl]^+$. Thus, obtaining the product is difficult because the counter ion of $[H(N{-}N)]^+$ prefers to form ion pairs with $[Ru(N{-}N)(CO)_3Cl]^+$. For this reason the full characterization of the protonated ion pairs could not be achieved. However they constitute evidence of the protonation of the phenanthroline ligands.

*$[Ru(CO)_3Cl_3]^-$ $[H(N{-}N)_1]^+$ (**10**)*

$(N{-}N)_1$ = 1, 10′-phenanthroline, ν(CO) = 2145, 2128, 2053 cm^{-1} in CH_2Cl_2. Anal. calcd, N 5.72%, C 36.79%, H 2.06%. Found, N 5.69%, C 36.40%, H 2.1%. This product crystallizes in very low quantity from the solution remaining after separation of products **1** and **7**. The structure was confirmed by X-ray crystallography.

*$[Ru(CO)_3Cl_3]^-$ $[H(N{-}N)_3]^+$ (**11**)*

$(N{-}N)_3$ = 2, 9′-dimethyl-1,10′-phenanthroline, ν(CO) = 2145, 2125, 2050 cm^{-1} in CH_2Cl_2. Anal. calcd, N 6.29%, C 40.51%, H 2.94%. Found, N 6.12%, C 40.20%, H 2.60%. $\delta_H(CDCl_3)$ 7.84d ($H_8{}^{8,7}J = 4.2$ Hz) 7.88s (H_5) 8.37d ($H_7{}^{7,8}J =$ 4.1 Hz) 3.25s (2,9′-CH_3). This product crystallizes in very low quantities from the solution remaining after separation of products **6** and **9**. The structure was confirmed by X-ray crystallography.

*$[Ru(CO)_3Cl_3]^-$ $[H(N{-}N)_2]^+$ (**12**)*

$(N{-}N)_2$ = 4, 7′-dimethyl-1,10′-phenanthroline, ν(CO) = 2144, 2130, 2055 cm^{-1} in CH_2Cl_2. This product crystallizes in very low quantities from the solution remaining after separation of products **3** and **8**. The structure was confirmed by X-ray crystallography

Synthesis of $[Ru(N_7)(CO)_3Cl_2]$ and $[Ru(CO)_3Cl_2]_2N_6$ (13) and (14)

N_7 = 2,4′-bipyridine, N_6 = 4,4′-bipyridine

These compounds were prepared following a published procedure.[58]

Synthesis of $[Ru(N{-}N)_5(CO)_2Cl(COOCH_3)]$, $[Ru(N{-}N)_5(CO)_2Cl(COOCH_2CH_3)]$ and $[Ru(CO)_3Cl_3]^-$ $[Ru(N{-}N)_5(CO)_3Cl]^+$ (15–17)

$N{-}N)_5$ = 2,2′-bipyridine

Complex **15** was prepared following a published procedure.[21] Complex **16** was prepared following a similar procedure to that for **15**, but using ethanol instead of methanol. Complex **17** was obtained following the same procedure as for complexes **7**–**9**. For complex **16**: colorless crystals, ν(CO) = 1633, 1993, 2057 cm^{-1} in CH_2Cl_2. $\delta_H(CDCl_3)$ 7.59t (H_4; $^{4,5}J = 7.5$ Hz, $^{4,3}J = 7.9$ Hz), 8.07t (H_5; $^{5,6}J = 4.5$ Hz), 8.22d (H_3; $^{3,4}J = 7.8$ Hz), 9.04d (H_6; $^{6,5}J = 4.5$ Hz),3.90q(CH_2 in alkoxy group $J = 10$ Hz), 1.1t(CH_3 in alkoxy group $J = 7$ Hz) $\delta_C(CDCl_3)$ 198.5 (COOR), 193.3 (CO), 155.5 (C_5), 153.5 (C_4), 139.7 (C_2), 127.4 (C_3), 123.5 (C_1), 60.0 (CH_3), 15.29 (CH_2). Anal. calcd, N 6.64%, C 42.71%, H 3.11%. Found, N 6.54%, C 42.57%, H 3.15%. Yield = 79%. For complex **17**: ν(CO) = 2143, 2125, 2091, 2075, 2050 cm^{-1} in CH_2Cl_2. $\delta_H(CDCl_3)$ 9.03d ($H_6{}^{6,5}J = 4.7$ Hz), 8.55d ($H_3{}^{3,4}J = 8$ Hz) 8.43t ($H_5{}^{5,4}$J = 7.5 Hz; ^{5,6}J = 4.5 Hz) 7.90t ($H_4{}^{4,5}$J = 7.5 Hz; ^{4,3}J = 7.9 Hz) $\delta_C(CDCl_3)$ 187.2 (CO), 156.5 (C_2), 155.8 (C_4), 143.7 (C_6), 130.2 (C_5), 126.5 (C_3). Anal. calcd N 4.19%, C 28.76%, H 1.21%. Found, N 4.21%, C 28.91%, H 1.21%. Yield = 68%.

Synthesis of $[Ru(CO)_3Cl_3]^-$ $[Ru(N{-}N)_4(CO)_3Cl]^+$ and $[Ru(N{-}N)_4(CO)_2Cl(COOCH_2CH_3)]$ (18 and 19)

$N{-}N)_4$ = 2,2′-bipyrimidine

Complex **18** was obtained following the same procedure as for complexes **7**–**9** in solution. For the dry reaction a 1 : 0.5 metal–ligand ratio was used. The reactants were mixed thoroughly in a mortar and the mixture was allowed to react. After a period of 1 h a change in color to deep yellow indicated that reaction has taken place Complex **19** was obtained as described for complexes **1**–**6**. For complex **18**: colorless crystals, ν(CO) = 2145, 2127, 2098, 2086, 2062, 2036 in KBr pellets. δ_H(DMSO) 8.11m, 9.31m. Anal. calcd, N 10.34%, C 27.72%, H 1.62%. Found, N 10.28%, C 27.43%, H 1.34%. Yield = 87%. For complex **19**: ν(CO) = 2059, 2004, 1624 cm^{-1} in KBr pellets. δ_H(DMSO) 8.07m, 9.30m, 3.90q(CH_2 in alkoxy group $J = 10$ Hz), 1.1t(CH_3 in alkoxy group $J = 7$ Hz). Anal. calcd, N 12.20%, C 34.0%, H 2.41%. Found, N 11.84%, C 33.80%, H 2.0%. Yield = 72%.

Table 1. Crystal data for compounds **1, 3–6, 10–12,16,18,20–23**

	1·(MeOH)	**3**	**4**	**5**	**6**	**10**	**11**
Empirical formula	$C_{17}H_{15}ClN_2O_5Ru$	$C_{18}H_{15}ClN_2O_4Ru$	$C_{19}H_{17}ClN_2O_4Ru$	$C_{18}H_{15}ClN_2O_4Ru$	$C_{20}H_{20}ClN_2O_{4.5}Ru$	$C_{15}H_{11}Cl_3N_2O_4Ru$	$C_{17}H_{13}Cl_3N_2O_3Ru$
Fw	463.83	459.84	473.87	459.84	496.90	490.68	500.71
Temperature (K)	120(2)	120(2)	120(2) K	293(2)	120(2)	120(2)	120(2)
λ(Å)	0.71073	0.71073	0.71073 Å	0.71073	0.71073	0.71073	0.71073
Cryst system	Triclinic	Triclinic	Orthorhombic	Triclinic	Triclinic	Monoclinic	Triclinic
Space group	P 1	P 1	Pbca	P 1	$P\bar{1}$	C2/c	P 1
a (Å)	8.7509(6)	8.2224(3)	10.6403(15)	8.0560(8)	8.0424(2)	28.5633(6)	9.1492(5)
b (Å)	10.0760(8)	9.8402(6)	14.553(3)	9.5392(12)	9.1378(3)	9.59990(10)	9.3348(4)
c (Å)	10.6053(7)	11.5170(7)	24.214(4)	11.9689(16)	13.9544(5)	12.7367(3)	11.5434(4)
α (deg)	88.502(4)	83.104(2)	90	91.197(11)	83.010(2)	90	101.601(3)
β (deg)	80.562(5)	76.240(3)	90	91.029(9)	81.094(2)	96.0620(10)	94.856(3)
γ (deg)	73.261(4)	74.61(3)	90	104.869(9)	76.217(2)	90	101.958(2)
V (Å^3)	883.15(11)	871.04(8)	3749.5(11)	888.53(19)	980.12(5)	3472.94(12)	936.53(7)
Z	2	2	8	2	2	8	2
ρ_{calc} (mg/m^3)	1.744	1.753	1.679	1.719	1.684	1.877	1.776
μ(Mo Kα) (mm^{-1})	1.070	1.080	1.006	1.059	0.968	1.387	1.284
R1[a] ($I \geq 2\sigma$)	0.0364	0.0288	0.0471	0.0201	0.0226	0.0224	0.0229
wR2[b] ($I \geq 2\sigma$)	0.0807	0.0648	0.0930	0.0503	0.0568	0.0518	0.0551

Table 1. Crystal data for compounds **1, 3–6, 10–12,16,18,20–23**

12	**16**	**18**·(CH_2Cl_2)	**20**	**21**	**22**	**23**·(CH_2Cl_2)
$C_{17}H_{13}Cl_3N_2O_3Ru$	$C_{15}H_{13}ClN_2O_4Ru$	$C_{15}H_8Cl_6N_4O_6Ru_2$	$C_{15}H_{15}ClN_2O_4Ru$	$C_8H_5Cl_2NO_3Ru$	$C_7H_4Cl_2N_2O_3Ru$	$C_{11}H_6Cl_6N_2O_6Ru_2$
500.71	421.79	755.09	423.81	335.10	336.09	677.02
120(2)	120(2)	100(2)	120(2)	100(2)	120(2)	100(2) K
0.71073	0.71073	0.71073	0.71073	0.71073	0.71073	0.71073 Å
Triclinic	Monoclinic	Monoclinic	Triclinic	Monoclinic	Monoclinic	Monoclinic
P 1	P $2_1/n$	P$2_1/c$	P 1	P $2_1/c$	P $2_1/c$	P $2_1/n$
8.5371(3)	7.9376(7)	11.5515(5)	7.8430(4)	9.9701(1)	9.0489(3)	5.8397(1)
10.5068(4)	11.8381(8)	10.1009(7)	8.8475(6)	19.4565(3)	8.8532(3)	17.9940(7)
12.6438(5)	17.4631(14)	21.7720(14)	13.0089(7)	12.5721(2)	13.9097(2)	9.7215(4)
65.935(2)	90	90	82.488(3)	90	90	90
78.088(2)	99.903(3)	91.878(4)	89.256(3)	110.2830(10)	103.963(2)	100.320(2)
67.353(2)	90	90	68.861(3)	90	90	90
954.06(6)	1616.5(2)	2539.0(3)	834.16(8)	2287.55(6)	1081.40(5)	1005.01(6)
2	4	4	2	8	4	2
1.743	1.733	1.975	1.687	1.946	2.064	2.237
1.261	1.155	1.859	1.119	1.821	1.929	2.331
0.0244	0.0396	0.0607	0.0211	0.0204	0.0220	0.0239
0.0583	0.0852	0.1366	0.0499	0.0442	0.0558	0.0511

[a] $R1 = \Sigma||F_o| - |F_c||/\Sigma|F_o|$.
[b] $wR2 = [\Sigma[w(F_o^2 - F_c^2)^2]/\Sigma[w(F_o^2)^2]]^{1/2}$.

Synthesis of $[Ru(py)_2(CO)_2Cl(COOCH_2CH_3)]$ (20)

py = pyridine

A 200 mg (0.39 mmol) aliquot of $[Ru(CO)_3Cl_2]_2$ was dissolved in 3 ml ethanol, 0.25 ml (3.09 mmol) of freshly distilled pyridine was added and the solution mixture was stirred overnight and place in the fridge. A white solid $[Ru(N_4)_2(CO)_2Cl(COOCH_2CH_3)]$, precipitates. The solid was filtered, washed with ethanol and dried under vacuum. Colorless crystals, ν(CO) = 1996, 2062, 2136 cm^{-1}. $\delta_H(CDCl_3)$ 8.78d ($H_{1,}H_{5;}$ $^{1,2}J = 2.5$ Hz), 7.84t (H_3; $^{3,2}J = 7.5$ Hz), 7.35t (H_2, H_4; $^{2,1}J = 2.5$ Hz, ^{2,3}J = 7.5 Hz), 4.13d (protons fromCH_2 J = 3.6 Hz), 3.719m, 1.42t (protons from CH_3; $J = 7$ Hz). Anal. calcd, N 6.61%, C 42.51%, H 3.57%. Found, N 6.54%, C 42.46%, H 3.56%. Yield = 75%.

Synthesis of $[Ru(py)(CO)_3Cl_2]$ (21)

The solvent was modified from the original procedure by Benedetti.[25] (py = pyridine). A 200 mg (0.39 mmol) aliquot of $[Ru(CO)_3Cl_2]_2$ was dissolved in 3 ml ethanol, 0.25 ml (3.09 mmol) of freshly distilled pyridine were added and the solution mixture was stirred overnight. Ethanol was evaporated and 1.5 ml of CH_2Cl_2 were added. A white precipitate formed. The solid was washed with ethanol and dried under vacuum. Colorless crystal; ν(CO) = 2051, 2075, 2136 cm^{-1}. $\delta_H(CDCl_3)$ 8.97d (H_1, H_5; $^{1,2}J = 2.5$ Hz), 8.00t (H_3; $^{3,2}J = 7.7$ Hz), 7.57t (H_2, $H_4^{2,1}$J = 2.5 Hz; $^{2,3}J = 7.5$ Hz). Anal. calcd, N 4.18%, C 28.67%, H 1.50%. Found, N 4.15%, C 28.72%, H 1.56%. Yield = 67%.

Synthesis $[Ru(CO)_3Cl_2(pz)]$ (22)

The solvent was modified from the original procedure by Dragonetti[59] (pz = pyrazine). A 200 mg (0.39 mmol) aliquot of $[Ru(CO)_3Cl_2]_2$ and 228 mg (2.84 mmol) of pyrazine was dissolved separately in 3 ml ethanol, the solutions were then combined and stirred overnight. A white precipitate formed, with yield = 96%. The solid was filtered and washed with ethanol and dried under vacuum. Colorless crystals, ν(CO) = 2055, 2080, 2139 cm^{-1} in CH_2Cl_2. δ_H(DMSO) 9.06dd (H_1,H_4; $^{1,3}J = 2.1$ Hz), 8.97 dd (H_2, H_3; $^{3,1}J = 2$ Hz). Anal. calcd, N 8.33%, C 25.02%, H 1.20%. Found, N 8.26%, C 24.99%, H 1.28%. Yield = 84%.

Synthesis of $[Ru(CO)_3Cl_2]_2(pz)$ (23)

pz = pyrazine

Preparation followed the same procedure as for $[Ru(CO)_3Cl_2(N_9)]$ but reducing the amount of pyrazine to 15 mg (0.195 mmol) to ensure that the dimer would form exclusively. Colorless crystals. δ_H(DMSO) 9.202 s%. Yield = 72%. Anal. calcd, N 4.73%, C 20.29%, H 0.68%. Found, N 5.03%, C 20.70%, H 1.08%.

Table 2. Calculated temperature corrected formation enthalpies

Reaction	Alkoxy carbonyl complexes	ΔH_f (kJ/mol)
$[Ru(CO)_3Cl_2]_2$ + 2 (1, 10′-phenanthroline) + 2MeOH	→ 2[Ru(1, 10′- phen)$(CO)_2$Cl(COOMe)] + 2HCl	−131.7
$[Ru(CO)_3Cl_2]_2$ + 2 (4, 7′-dimethyl-1, 10′-phenanthroline) + 2EtOH	→ 2[Ru(4, 7′-dimethyl-1, 10′-phen)$(CO)_2$Cl(COOEt)] + 2HCl	−145.1
$[Ru(CO)_3Cl_2]_2$ + 2 (2, 9′-dimethyl-1, 10′-phenanthroline) + 2MeOH	→ 2[Ru2, 9′-dimethyl-1, 10′-phen)$(CO)_2$Cl(COOMe)] + 2HCl	−95.1
$[Ru(CO)_3Cl_2]_2$ + 2 (2, 9′-dimethyl-1, 10′-phenanthroline) + 2EtOH	→ 2[Ru(2, 9′-dimethyl-1, 10′-phen)$(CO)_2$Cl(COOEt)] + 2HCl	−88.7
$[Ru(CO)_3Cl_2]_2$ + 2(4, 7′-dimethyl-1, 10′-phenanthroline) + 2MeOH	→ 2[Ru(4, 7′-dimethyl-1, 10′-phen)$(CO)_2$Cl(COOMe)] + 2HCl	−146.9
$[Ru(CO)_3Cl_2]_2$ + 2 (1, 10′-phenanthroline) + 2EtOH	→ 2[Ru(1, 10′-phen)$(CO)_2$Cl(COOEt)] + 2HCl	−109.1
$[Ru(CO)_3Cl_2]_2$ + 2 (2, 2′-bipyrimidine) + 2EtOH	→ 2[Ru(2, 2′-bpmd)$(CO)_2$Cl(COOEt)] + 2HCl	−100.5
$[Ru(CO)_3Cl_2]_2$ + 4 pyridine + 2MeOH	→ 2[Ru$(py)_2$ $(CO)_2$Cl(COOMe)] + 2HCl	−158.3
$[Ru(CO)_3Cl_2]_2$ + 4 pyridine + 2EtOH	→ 2[Ru$(py)_2(CO)_2$Cl(COOEt)] + 2HCl	−150.1
	Non-alkoxy carbonyl complexes	
$[Ru(CO)_3Cl_2]_2$ + 2 (2, 4′-bipyridine)	→ 2[Ru(2, 4′-bpy)$(CO)_3Cl_2$]	−92.0
$[Ru(CO)_3Cl_2]_2$ + 2(4, 4′-bipyridine)	→ 2[Ru(4, 4′-bpy)$(CO)_3Cl_2$]	−73.4
$[Ru(CO)_3Cl_2]_2$ + 4, 4′-bipyridine	→ $[Ru(CO)_3Cl_2]_2$(4, 4′-bpy)	−66.9
$[Ru(CO)_3Cl_2]_2$ + 2 pyridine	→ 2[Ru(py)$(CO)_3Cl_2$]	−77.0
$[Ru(CO)_3Cl_2]_2$ + 2 pyrazine	→ [Ru(pz)$(CO)_3Cl_2$]	−52.5
$[Ru(CO)_3Cl_2]_2$ + pyrazine	→ $[Ru(CO)_3Cl_2]_2$(pz)]	−40.8

Table 3. Catalytic activity for the hydroformylation of 1-hexene by the ruthenium catalysts

Catalyst	Percentage conversion	Percentage 1-hexene	Percentage hexane	Percentage isomers	Percentage aldehydes	Percentage alcohols
[Ru(1,10′-phen)$(CO)_2$Cl ($COOCH_3$)] (**1**)	0	100	0	0	0	0
[Ru(4,7′-dimethyl-1,10′-phen)$(CO)_2$Cl ($COOCH_2CH_3$)] (**2**)	0	100	0	0	0	0
[Ru(2,9′-dimethyl-1,10′-phen)$(CO)_2$Cl($COOCH_3$)] (**5**)	0	100	0	0	0	0
[Ru(4,7′-dimethyl-1,10′-phen)$(CO)_2$Cl($COOCH_3$)] (**3**)	0	100	0	0	0	0
[Ru(1,10′-phen)$(CO)_2$Cl($COOCH_2CH_3$)] (**2**)	0	100	0	0	0	0
[Ru(2,9′-dimethyl-1,10′-phen)$(CO)_2$Cl($COOCH_2CH_3$)] (**6**)	0	100	0	0	0	0
[Ru(2,2′-bpmd)$(CO)_3$Cl($COOCH_2CH_3$)] (**18**)	0	100	0	0	0	0
[Ru(2,2′-bpmd)$(CO)_3$Cl]$^+$[Ru$(CO)_3Cl_3$]$^-$ (**19**)	9	91	0	9	0	0
[Ru(2,2′-bpy)$(CO)_2$Cl($COOCH_3$)] (**15**)	10	90	0	0	0	10
[Ru(2,2′-bpy)$(CO)_2$Cl($COOCH_2CH_3$)] (**16**)	28	72	0	16	0	12
[Ru(2,4′-bpy)$(CO)_3Cl_2$] (**13**)	46	54	0	13	27	6
$[Ru(CO)_3Cl_2]_2$(4,4′-bpy) (**14**)	47	53	0	18	9	20
$[Ru(CO)_3Cl_2]_2$(pz) (**23**)	45	51	0	13	10	22
[Ru(pz)$(CO)_3Cl_2$] (**22**)	67	33	0	32	27	8
[Ru(py)$(CO)_3Cl_2$] (**21**)	86	15	0	15	51	20
[Ru$(py)_2(CO)_2$Cl($COOCH_2CH_3$)] (**20**)	83	17	0	12	49	22
$[Ru(CO)_3Cl_2]_2$	97	3	0	26	41	30

Conditions: $T = 120\,^{\circ}C$; reaction time = 17 h; n(Ru) = 0.16 mmol; V(solvent) = 5 ml 1-methyl-2-pyrrolidone; V(1-hexene) = 0.5 ml; V(standard) = 0.2 ml cyclohexane. CO : H_2 1 : 1 20 bar.

Table 4. Calculated natural bite angles and proton affinities for the free ligands. Complexation energies for the coordinated ligands

Ligand	
	Proton affinity (kJ/mol)
2,4′-Bipyridine	974
4,4′-Bipyridine	945
Pyridine	939/925[a]
Pyrazine	883/887[b]
	Natural bite angle (deg)
1,10′-Phenanthroline	83.02
4,7′-Dimethyl-1,10′-phenanthroline	82.76
2,9′-Dimethyl-1,10′-phenanthroline	82.73
2,2′-Bipyrimidine	81.89
2,2′-Bipyridine	81.77
Complex	*Association energy (kJ/mol)*
Ru-1,10′-phenanthroline	−328
Ru-2,2′-bipyridine	−280
Ru-2,2′-bipyrimidine	−260
Ru-pyrazine	−238
Ru-pyridine	−180

[a,b] Experimental values for proton affinities in kJ/mol.[47]

X-ray structure determinations

The X-ray diffraction data of **5** was collected with a Nonius Mach3 diffractometer using Mo Kα radiation ($\lambda = 0.71073$ Å). Cell parameters were obtained from 25 automatically centered reflections. Intensities were corrected for background, polarization and Lorentz effects. CAD4-Express and XCAD4-Express programs[60–62] were used for cell refinement and data reduction. All other data collections were carried out by Nonius KappaCCD diffractometer. The Denzo-Scalepack[63] program package was used for cell refinements and data reduction for these data sets. Structures were solved by direct methods using the SHELXS-97, SIR-97 or SIR-2002 programs or by the Patterson heavy atom method (**9** and **14**) using the DIRDIF-99 program.[63–66] A multiscan absorption correction based on equivalent reflections (XPREP in SHELXTL version 6.12)[67] was applied to all data except for **5** (T_{min}/T_{max} values were 0.8145/0.9005, 0.8130/0.8997, 0.8241/0.9514, 0.7206/0.8763, 0.5710/0.5760, 0.6810/0.8737, 0.6993/0.7832, 0.7035/0.8843, 0.8932/0.9445, 0.6318/0.8374, 0.6195/0.8764, 0.6129/0.8332, 0.6151/0.8455 and 0.6845/0.9064, for **1**, **3–6**, **10–12**, **16**, **18** and **20–23** respectively). All structures were refined with SHELXL-97[68] and WinGX graphical user interface.[69] In structure **2** the OH hydrogen of MeOH was located from the difference Fourier map but not refined. In **10–12** all hydrogens were located from the difference Fourier map and refined isotropically. In **6** the ethanol solvent was disordered over two sites with equal occupation parameter 0.5. The OH hydrogen of the ethanol solvent was located from the difference Fourier, but in the final refinement defined as a riding atom. The CH_3 and CH_2 hydrogens of the EtOH solvent were omitted. The water hydrogens in **10** were refined with equal U_{iso}. All other hydrogens were placed in idealized position and constrained

to ride on their parent atom. The crystallographic data for **1**, **3–6**, **10–12**, **16**, **18** and **20–23** are summarized in Table 1. Selected bond lengths and angles for structures **4, 11, 18, 20, 22** and **23** are shown in the figure captions. The thermal ellipsoid plot of structures **1, 3, 5–7, 10–12, 16** and **21** are given as supplementary material. The structure solution of ruthenium acetonitrile complex $[Ru(CO)_3(CH_3CN)Cl_2]$ (**24**) was unsatisfactory. However, the structure provided further evidence of the formation of the acetonitrile derivative and therefore the crystallographic details are given in the supplementary section.

Catalysis

The hydroformylation reactions were performed in high-pressure autoclaves (100 ml Berghof) equipped with a Teflon liner. The autoclaves were charged in a glove box. In a typical experiment the solvent 1-methyl-2-pyrrolidinone (5 ml), the standard cyclohexane (0.5 ml), the olefin 1-hexene (0.2 ml) and the catalyst were added to the autoclave, which was then pressurized to 20 bar with synthesis gas $CO:H_2$, 1:1. The autoclave was heated at 120 °C for 17 h. The reaction was then stopped and the autoclave was rapidly cooled to room temperature and brought to atmospheric pressure, after which the liquid samples were analyzed. The product distribution is reported as weight-percent.

The gases CO and H_2 used in the hydroformylation experiments were of 99 and 99.99% purity, respectively. The solvent 1-methyl-2-pyrrolidone (Aldrich, 99%) and the internal standard cyclohexane (Merck, 99%) were used without further purification and degassed with nitrogen before use. Similarly, 1-hexene (99%) was degassed prior to use.

Gas chromatographic analyses of the product mixture were recorded on a Hewlett-Packard 5890 series II chromatograph equipped with a Varian WCOT fused silica 50×0.53 m column and temperature programming.

Computational details

The geometries of the complexes were optimized using the B3PW91 hybrid density functional method and employing 6-31G* as a basis set (for ruthenium, Huzinaga's extra basis 433321/4331/421[70]). The geometry optimizations were followed by analytical frequency calculations to obtain the vibration spectra and stationary point of all compounds. The calculations were carried out using Gaussian-98 for the natural bite angles and association energies and Gaussian03 for the formation enthalpies and proton affinities. The basis set superposition error (BSSE) correction was estimated using the counterpoise method. Natural bite angles were calculated at DFT level by optimizing the metal nitrogen-containing fragment excluding the other ligands coordinated to the metal center using Stuttgart ECP basis set for ruthenium and p-0.081 polarization function. All reactions were modeled in the gas phase.

Acknowledgments

The authors would like to thank Taina Nivajärvi for her valuable help in obtaining crystalline samples of some of the coordinated complexes, and Dr Pipsa Hirva for her contribution and valuable comments on the molecular modeling calculations. Financial support provided by the Academy of Finland is gratefully acknowledged (M.H.).

Supplementary information

CCDC-264 250 (**1**), CCDC-264 251 (**3**), CCDC-264 252 (**4**), CCDC-264 253 (**5**), CCDC-264 254 (**6**), CCDC-264 255 (**7**), CCDC-264 256 (**10**), CCDC-264 257 (**11**) CCDC-264 258 (**12**), CCDC-264 259 (**16**), CCDC-264 260 (**18**), CCDC-264 261 (**20**), CCDC-264 262 (**21**), CCDC-264 263 (**22**), CCDC-264 264 (**23**), CCDC-264 265 (**24**) contain the supplementary crystallographic data for this paper. These data can be obtained free of charge from The Cambridge Crystallographic Data Centre via www.ccdc.cam.ac.uk/data_request/cif.

REFERENCES

1. Eskelinen E, Haukka M, Kinnunen TJ, Pakkanen TA. *J. Electroanal. Chem.* 2003; **556**: 103–108.
2. Eskelinen E, Haukka M, Kinnunen TJ, Pakkanen TA. *Eur. J. Inorg. Chem.* 2002; **5**: 1169–1173.
3. O'Reagan B, Grätzel M. *Nature* 1991; **353**: 737–740.
4. Grätzel M. *Platinum Metals Rev.* 1994; **38**: 151–159.
5. Nazeeruddin MK, Kay A, Rodicio I, Humphry-Baker R, Müller E, Liska P, Vlachopoulus N, Grätzel M. *J. Am. Chem. Soc.* 1993; **115**: 6382–6390.
6. Yamaguchi T, Imai N, Ito T, Kubiak CP. *Bull. Chem. Soc. Jap.* 2000; **73**(5): 1205–1212.
7. Ng Y, Chi-Ming C, Peng SM. *N. J. Chem.* 1996; **20**(7–8): 781–787.
8. Chen Y, Shepherd RE. *Inorg. Chem.* 1998; **37**: 1249–1256.
9. Londergan CH, Kubiak CP. *J. Phys. Chem. A.* 2003; **107**: 9301–9311.
10. Yamagushi T, Kido H, Zavarine IS, Richmond T, Washignton J, Kubiak CP. *J. Am. Chem. Soc.* 1999; **121**: 4625–4632.
11. Braun-Sand SB, Wiest O. *J. Phys. Chem. A* 2003; **107**: 285–289.
12. Mujica V, Nitzan A, Datta S, Ratner MA, Kubiak CP. *J. Phys. Chem. B* 2003; **107**: 91–95.
13. Cetinkaya B, Cetinkaya E, Brookhart M, White PS. *J. Mol. Catal. A* 1999; **142**: 101–112.
14. Bianchini C, Lee HM. *Organometallics.* 2000; **19**: 1833–1840.
15. Luukkanen S, Haukka M, Kallinen M, Pakkanen TA. *Cat. Lett.* 2000; **70**: 123–125.
16. Tanaka K, Mizukawa T. *Appl. Organometal. Chem.* 2000; **14**: 863–866.
17. Chardon-Noblat S, Deronzier A, Ziessel R, Zsoldos D. *Inorg. Chem* 1997; **36**: 5384–5389.
18. Lorkovic IM, Miranda KM, Lee B, Bernhard S, Shoonover JR, Ford PC. *J. Am. Chem. Soc.* 1998; **120**: 11 674–11 683.
19. Sauaia MG, de Lima RG, Tedesco AC, da Silva RS. *J. Am. Chem. Soc.* 2003; **125**: 14 718–14 719.
20. Haukka M, Kiviaho J, Ahlgren M, Pakkanen TA. *Organometallics* 1995; **14**(2): 825–833.
21. Luukkanen S, Haukka M, Pakkanen TA. *Inorg. Chim. Acta* 2000; **309**: 155–158.
22. Haukka M, Hirva P, Luukkanen S, Kallinen M, Ahlgren M, Pakkanen TA. *Inorg. Chem.* 1999; **38**: 3182–318.
23. Bruce MI, Stone FGA. *J. Chem. Soc. A* 1967; 1238–1243.
24. Johnson BFG, Johnston RD, Lewis J. *J. Chem. Soc. A* 1969; 792–796.

25. Benedetti E, Braca G, Sbrana G, Salvetti F, Grassi B. *J. Organometal. Chem.* 1972; **37**: 361–373.
26. Garlaschelli L, Martinengo S, Chini P. *J. Organometal. Chem.* 1981; **213**: 379–388.
27. Garlaschelli L, Malatesta MC, Martinengo S, Demartin F, Manassero M, Sansoni M. *J. Chem. Soc., Dalton Trans.* 1986; **4**: 777–782.
28. Ciani G, Sironi A, Chini P, Martinengo S. *J. Organometal. Chem.* 1981; **213**: C37–40.
29. Gusev OV, Morozova LN, Peganova TA, Antipin MY, Lyssenko KA, Noels AF, O'Leary SR, Maitlis PM. *J. Organometal. Chem.* 1997; **536**: 191–196.
30. Suss-Fink G, Soulie JM, Rheinwald G, Stoeckli-Evans H, Sasaki Y. *Organometallics* 1996; **15**: 3416–3422.
31. Andreu PL, Cabeza JA, Pellinghelli MA, Riera V. *Inorg. Chem.* 1991; **30**: 4611–4616.
32. Olmstead WN, Margolin Z, Bordwell FG. *J. Org. Chem.* 1980; **45**: 3295–3299.
33. Bartzatt R. *J. Biochem. Biophys. Meth.* 2001; **47**: 189–19.
34. Kabashima H, Hattori H. *Catal. Today.* 1998; **44**: 277–283.
35. Vila A, Mosquera RA. *Chem. Phys. Lett.* 2000; **332**: 474–480.
36. Raczynska ED. *J. Mol. Struct.* 1998; **427**: 87–96.
37. Oswald IDH, Allan DR, McGregor PA, Motherwell WDS, Parsons S, Pulham CR. *Acta Crystallogr. B* 2002; **58**: 1057–1066.
38. Johnson BFG, Lewis J, Nelson WJH, Nicholls N, Vargas MD, Bragga D, Henrick K, McPartlin M. *J. Chem. Soc. Dalton. Trans.* 1984; **4**: 1809–1814.
39. Hong KK, Wong WT. *Inorg. Chem.* 1996; **35**: 5393–5395.
40. Berg A, Dehnicke K, Fenske D. *Z. Anorg. Allg. Chem.* 1985; **527**: 111–117.
41. Teulon P, Roziere J. *Z. Anorg. Allg. Chem.* 1981; **483**: 219–224.
42. Griffith CS, Koutsantonis GA, Raston CL, Selegue JP, Skelton BW, White AH. *J. Organometal. Chem.* 1996; **518**: 197–202.
43. Oresmaa L, Haukka M, Vainiotalo P, Pakkanen TA. *J. Org. Chem.* 2002; **67**: 8216–8219.
44. Lau TC, Kochi JK. *J. Chem. Soc. Chem. Commun.* 1987; **11**: 798–799.
45. Haukka M, Alvila L, Pakkanen TA. *J. Mol. Cat. A Chem.* 1995; **102**: 79–92.
46. Frediani P, Bianchi M, Salvini A, Carluccio L, Rosi L. *J. Organomet. Chem.* 1997; **547**: 35–40.
47. Kunz R, Dinatale W, Becotte-Haigh P. *Int. J. Mass Spectrom.* 2003; **226**: 379.
48. Casey CP, Whiteker GT. *Isr. J. Chem.* 1990; **30**: 299–304.
49. Casey CP, Whiteker GT, Melville MC, Petrovich LM, Gavney JA, Powell DR. *J. Am. Chem. Soc.* 1992; **114**: 5535–5543.
50. Kranenburg M, van der Burgt YEM, Kamer PCJ, van Leeuwen PWNM. *Organometallics* 1995; **14**: 3081–3089.
51. Lau C-P, Cheng L. *J. Mol. Catal.* 1993; **84**: 39–50.
52. Jia G, Lin Z, Lau C-P. *Eur. J. Inorg. Chem.* 2003; 2551–2562.
53. Childs GI, Cooper AI, Nolan TF, Carrot MJ, George MW, Poliakoff M. *J. Am. Chem. Soc.* 2001; **123**: 6857–6866.
54. Sanchez-Delgado RA, Bradley JS, Wilkinson G. *J. Chem. Soc., Dalton Trans.* 1976; 399–404.
55. Sanchez-Delgado RA, Thewalt U, Valencia N, Andriollo A, Marquez-Silva R-L, Puga J, Schollhorn H, Klein H-P. *Inorg. Chem.* 1986; **25**: 1097–1106.
56. Salvini A, Frediani P, Rovai D, Bianchi M, Piacentti F. *J. Mol. Catal.* 1994; **89**: 77–92.
57. Khan MMT, Rao NS, Halligudi SB. *J. Mol. Catal.* 1990; **63**(2): 137–146.
58. Kinunen T, Haukka M, Pesonen E, Pakkanen TA. *J. Organometal. Chem.* 2002; **655**: 31–38.
59. Dragonetti C, Pizzotti M, Roberto D, Galli S. *Inorg. Chim. Acta* 2002; **330**: 128–135.
60. *CAD4 Express Software.* Enraf–Nonius: Delft, 1994.
61. Harms K, Wocadlo S. *XCAD4–CAD4 Data Reduction.* University of Marburg: Marburg, 1995.
62. Otwinowski Z, Minor W. *Processing of X-ray Diffraction Data Collected in Oscillation Mode. Methods in Enzymology, Volume 276, Macromolecular Crystallography, Part A*, Carter Jr CW, Sweet RM (eds). Academic Press: New York, 1997; 307–326.
63. Sheldrick GM. *SHELXS97, Program for Crystal Structure Determination*. University of Göttingen: Göttingen, 1997.
64. Altomare A, Burla MC, Camalli M, Cascarano GL, Giacovazzo C, Guagliardi A, Moliterni AGG, Polidori G, Spagna RJ. *Appl. Crystallogr.* 1999; **32**: 115–120.
65. Burla MC, Camalli M, Carrozzini B, Cascarano GL, Giacovazzo C, Polidori G, Spagna RJ. *Appl. Crystallogr.* 2003; **36**: 1103–1109.
66. Beurskens PT, Beurskens G, de Gelder R, Garcia-Granda S, Gould RO, Israel R, Smits JMM. *The DIRDIF-99 Program System.* Crystallography Laboratory, University of Nijmegen: Nijmegen, 1999.
67. Sheldrick GM. *SHELXTL v. 6.14.* Bruker Analytical X-ray Systems, Bruker AXS Inc.: Madison, WI, 2003.
68. Sheldrick GM. *SHELXL97, Program for Crystal Structure Refinement.* University of Göttingen: Göttingen, 1997.
69. Farrugia LJJ. *Appl. Crystallogr.* 1999; **32**: 837–842.
70. Huzinaga S (ed.). *Gaussian Basis Sets for Molecular Calculations. Physical Sciences Data* 16. Elsevier: Amsterdam, 1984.